SPECTRAL METHODS

B. Machenhauer
Danish Meteorological Institute
Copenhagen Denmark

1. INTRODUCTION

From the start of numerical weather prediction in the fifties, there has been a steady increase in the sophistication of mathematical models of the behaviour of the atmosphere, with both a progressive reduction of the approximations used in the equations and a progressive refinement of the resolution of the models. These developments have been closely linked with increases in computing power. In parallel there has also been a steady increase in sophistication and accuracy due to improvement of the numerical techniques used to discretize the continuous equations of the mathematical models. This has been the result of a major research effort carried out in many countries. The weight of these efforts bore on both spatial and temporal discretisation techniques. We shall here concentrate on the former. Until 1972 almost all numerical models were based on finite-difference (grid-point) techniques and much of the effort was spent on them. Other techniques were regarded more as mathematical recreation than as realistic potential alternatives for operational forecast or general circulation models. However, in the following years there were a renewed interest of other techniques and a rapid development took place. In particular of two of them, namely finite-element methods (which have been widely used in many other sectors of fluid dynamics) and spectral methods (which also have been used in several fields of theoretical and applied physics). We shall be concerned with the spectral method which are now the most widely used spatial discretisation method in global meteorological models.

We shall postpone a description of the historical events that lead to this stage and just mention here that a breakthrough was the adaption of transform methods to numerical spectral models worked out independently by *Eliassen et al.* (1970) and *Orszag* (1970): the idea is to evaluate all main quantities at the nodes of an associated grid where all non linear terms can then be computed as in a classical grid point model, thereby making possible the inclusion of physical processes in a straightforward way. The method also considerably reduced the requirements for storage and computations, and it then became possible to envisage spectral models with higher resolutions and an efficiency at least comparable with that of the most efficient grid point models of equivalent accuracy, that were used operationally. The first countries that implemented spectral models for routine forecasts were Australia and Canada in 1976, USA (NMC) in 1980, France in 1982 and Japan and ECMWF in 1983. In each case the grid point model used previously and the spectral model that replaced it were

compared with respect to performance and efficiency. The most extensive and clean comparison performed were that carried out at ECMWF by *Girard and Jarraud* (1982) and *Jarraud and Girard* (1984) which showed clearly that on the average increased performance were obtained with the spectral model, when compaired with the grid point model using the same computing time and a larger core storridge. At present also most research groups involved in general circulation studies and climate simulations use spectral models since this technique has proved most efficient and easy to implement for long global integrations.

So less than twenty years after the introduction of the first primitive equation multi-level spectral model (*Bourke*, 1974) this technique has become the most widely used numerical tool for treating the horizontal part of the equations in hemispheric or global problems. However, this does not mean that they represent the ultimate step in numerical techniques for weather prediction: other techniques are being developed, or may be developed in the future, which could turn out to more more efficient methods for a comparable accuracy.

As the primally goal of the ECMWF Seminars is the education of member state meteorologists I found it natural to base the present paper on the chapter that I wrote on "The Spectral Method" in the WMO text book on "Numerical Methods used in Atmospheric Models" (*Machenhauer*, 1979). To some extend the present paper is a shortened version of the text book chapter (which may be seen from some missing equation numbers as I have kept the same numbering of the equations in both papers). Rather than trying to make a complete review the emphasis is placed on basic principles and properties of spectral methods and on a description of alternative computational techniques that have been and are beeing used in global models. For more extensive reviews the reader is referred to those of *Bourke et al.* (1977), *Orszag* (1979) and *Jarraud and Simmons* (1984) and concerning the formulation and performance of the ECMWF model to the contributions by *H. Hortal and A. Simmons* to these proceedings.

The present paper is organised as follows. In Section 2 the basic principles upon which spectral methods are based are presented, and in Section 3 the basic properties of the methods are illustrted by application to the one-dimensional advection equation. The spectral techniques applied to models in spherical geometry are finally treated in Section 4.

2. BASIC PRINCIPLES

The complete set of equations used in any atmospheric model may quite generally be written in the form

$$\frac{\partial}{\partial t}\mathcal{L}_i(\omega^i) = F_i(\omega^1,\omega^2, \ldots\ldots,\omega^I) \quad ; \quad i = 1,2, \ldots,I. \qquad (2.1)$$

where the prognostic variables $\omega^i = \omega^i(\vec{r},t)$, i=1,2,...,I, are scalar functions of the space coordinates, given by $\vec{r}$, and the time t. F_i a function of the prognostic variables generally including linear as well as nonlinear terms which involves space derivatives and in some models even space integrals. In F_i the diagnostic variables are supposed to be eliminated by means of the diagnostic equations of the model. $\mathcal{L}_i$ is a space differential operator which in most cases becomes the identity operator, i.e. $\mathcal{L}_i(\omega_i) \equiv \omega_i$. In models in which the vorticity in the divergence equation is used the stream function and the velocity potential may be used as prognostic variables in which case $\mathcal{L}_i(\omega_i) \equiv \nabla^2(\omega_i)$ for these equations. Here ∇^2 is the horizontal Laplacian operator. We shall refer to the system of equations (2.1) as the partial differential model equations.

In the numerical solution of the partial differential model equations different numerical methods may be used. In the grid point method, the spatial dependence of the variables is represented by values at discrete points in physical space and derivatives and integrals are approximated by finite difference and quadrature formulae.

An alternative approach is to approximate the field of any dependent variable at a certain time by a finite series expansion in terms of linearly independent analytical functions, $\Psi_n(\vec{r})$, which are defined over the whole continuous integration region S. Thus any of the variables ω^i is approximated by a series of the form

$$\hat{\omega}^i(\vec{r},t) = \sum_{n=1}^{N} \omega_n^i(t)\psi_n(\vec{r}), \qquad (2.2)$$

where N is a constant positive integer. Using such a representation space derivatives and integrals can be evaluated analytically so that no finite space difference approximations or quadrature formulae are explicitly needed. The representation (2.2) is, however, equivalent to a representation in terms of the values of ω^i in N grid points distributed over the region and the use of (2.2) as an interpolating function fitting exactly in all N grid points. Evaluation of space derivatives and integrals using (2.2)

may therefore be considered as equivalent to the use of certain finite differences and quadratures on this grid. With the expansion functions used in practice these finite differences and quadratures are generally of a higher degree of accuracy than those usually used in the grid point method.

We shall call a method built upon a representation of the form (2.2) a series expansion method. The spectral method and the pseudo-spectral method, to be considered in this chapter, as well as the finite element method considered in a following chapter are all series expansion methods. In such methods the time dependence of the prognostic variables is determined by the expansion coefficients, that is by the values of $\omega_n^i(t)$, and consequently the methods involve the transformation of the partial differential model equations into a system of ordinary differential equations which determine the time derivatives of the expansion coefficients in the finite series. This transformation is analogous to the transformation carried out in the grid point method when the system of equations determining the time derivatives of the grid point values is constructed. Thus, when a series expansion method is used as well as when a grid point method is used a finite set of ordinary differential equations is obtained. We shall call these equations the space truncated model equations. In numerical models utilizing a series expansion method a discrete representation in time is used as in grid point models.

A finite series representation of the form (2.2) can only be an exact solution to the partial differential model equations in very special cases (e.g. when F_i is linear in the variables ω^i), therefore the transformation of the partial differential model equations to the space truncated equations must in general involve some approximations. These approximations are minimized by determining the transformed system of equations subject to some "best fit" criterion. It is in the choice of "best fit" that the spectral method and the pseudo-spectral method differ. The spectral method is based on a least square approximation, which as we shall see is equivalent to a so-called Galerkin approximation, whereas the pseudo-spectral method forces the mathematical equations to be exactly satisfied in a number of grid points equal to the number of expansion coefficients (the collocation method). In the finite element method either of the approximations may be used, but quite different expansion functions are used. Here we shall consider only the transformation procedure when based on a least square criterion.

In order to simplify the presentation let us consider a model with only one variable, ω. (The following presentation may easily be extended to the case with more prognostic variables). Equations (2.1) are then reduced to

$$\frac{\partial}{\partial t}\mathcal{L}(\omega) = F(\omega) \tag{2.3}$$

and the initial conditions become

$$\omega(\vec{r},0) = f(\vec{r}). \tag{2.4}$$

In order to avoid problems connected with complicated boundary conditions we shall furthermore assume that these are of a type which can be satisfied by a proper choice of the expansion functions for any truncation of the approximate solution

$$\hat{\omega}(\vec{r},t) = \sum_{n=1}^{N} \omega_n(t)\, \Psi_n(\vec{r}) \tag{2.5}$$

an for any set of the expansion coefficients. As we shall see this is the case in the applications of the spectral method to be considered in the following.

The space truncated equations are now derived by minimizing the mean square integral of the residue $R(\tilde{\omega}) = \partial\mathcal{L}(\tilde{\omega})/\partial t - F(\tilde{\omega})$, obtained by substituting (2.5) into (2.3) That is, at any time we choose those values of $d\omega_n/dt$ which minimize

$$J(\hat{\omega}) = \int_S \left(\sum_{n=1}^{N} \frac{d\omega_{n'}}{dt}\mathcal{L}(\Psi_n) - F\left(\sum_{n=1}^{N} \omega_n \Psi_n\right)\right)^2 dS.$$

These values are obtained by setting the derivatives of $J(\tilde{\omega})$ with respect to $d\omega_n/dt$ equal to zero (the condition for a minimum) and the resulting space truncated equations become

$$\int_S \left(\sum_{n'=1}^{N} \frac{d\omega_{n'}}{dt}\mathcal{L}(\Psi_{n'}) - F\left(\sum_{n'=1}^{N} \omega_{n'}\Psi_{n'}\right)\right) \mathcal{L}(\Psi_n) dS = 0 \tag{2.6}$$

$$\text{for } n = 1,2,.....N.$$

We note that (2.6) may be written as

$$\int_S R(\hat{\omega})\, \Psi_n dS = 0 \quad \text{for } n = 1,2, \ldots,N \tag{2.7}$$

if

$$\mathcal{L}(\Psi_n) + \epsilon_n \Psi_n = 0 \quad \text{for } n = 1,2, \ldots,N, \tag{2.8}$$

where ϵ_n are constants. When $\mathcal{L}$ is the identity operator (2.8) is satisfied by any set of expansion functions Ψ_n (with ϵ_n = -1 for all n). When $\mathcal{L}$ is different from the identity operator (2.8) implies that the expansion functions are eigensolutions of the $\mathcal{L}$ operator.

The system of equations (2.7) could have been written down immediately by making use of the Galerkin approximation with Ψ_n as test functions (*Galerkin*, 1915). Namely, by forcing the residue $R(\tilde{\omega})$ to be zero in an averaged sense over domain S with the expansion functions Ψ_n as weights. The above derivation, however, shows that the Galerkin approximation is equivalent to a least square approximation, when applied to equations of the form used in atmospheric models, and when the expansion functions satisfy the condition (2.8).

We note an important property of the transformed system of equations (2.7), which is a consequence of the Galerkin approximation. Namely, that the residue $R(\tilde{\omega})$ becomes orthogonal to $\hat{\omega}$

$$\int_S R(\hat{\omega})\ \hat{\omega}\ dS = 0\ . \tag{2.9}$$

This is easily obtained by multiplying each of the equations in the system (2.7) by the corresponding coefficient ω_n and adding all the resulting equations. We shall see that this property is essential for certain integral properties of the transformed systems.

Assuming the conditions (2.8) to be satisfied we write the system (2.6) in a form suitable for a numerical integration

$$\sum_{n'=1}^{N} \epsilon_{n'} I_{nn'} \frac{d\omega_{n'}}{dt} = -\int_S F\left(\sum_{n'=1}^{N} \omega_{n'} \Psi_{n'}\right) \Psi_n dS \tag{2.10}$$

$$\text{for } n = 1,2,\ldots,N\ ,$$

where $$I_{nn'} = \int_S \Psi_n \Psi_{n'}\ dS\ .$$

It is seen that this space truncated system of equations is a nonhomogeneous system of N linear algebraic equations with constant coefficients $\epsilon_n, I_{nn'}$, which can be computed once and for all, and with the N unknowns $d\omega_n/dt$. Suppose now that the expansion coefficients $\omega_n(t)$ are known at a certain time, then the values of the right-hand sides may be computed and by solving the system of equations the values of $d\omega_n/dt$ may be determined. Thus, if initial values of the expansion coefficients are given, a numerical integration may be carried out by the use of some time differencing scheme. The initial values of ω_n must be obtained from a given initial field of the form (2.4).

Generally this field cannot be represented exactly by a truncated series expansion, so that some "best fit" criterion must be applied. A logical choice of this criterion is of course the one upon which the numerical method is based. That is, to determine the initial values of the coefficients to be those minimizing the mean square deviation

$$\int_S (\omega(\vec{r},0) - \hat{\omega}(\vec{r},0))^2 \, dS$$

which leads to the system of equations

$$\sum_{n'=1}^{N} I_{nn'} \, \omega_{n'}(0) = \int_S \omega(\vec{r},0)\Psi_n(\vec{r}) \, dS \qquad (2.11)$$

$$\text{for } n = 1,2,\ldots,N .$$

In the case of "real" initial data the values of $\omega(\vec{r},0)$ are usually determined from observations by some objective analysis scheme only in a finite set of discrete points and the right-hand side may then be evaluated by some quadrature formulae.

The determination of the initial values of ω_n and of the tendencies $d\omega_n/dt$ in a certain time step from the systems of equations (2.10) and (2.11) generally involves matrix inversions. the inversions can, however, be avoided by choosing functions which are orthogonal, that is, functions satisfying the conditions

$$I_{nn'} = \int_S \Psi_n(\vec{r}) \, \Psi_{n'}(\vec{r}) \, dS = 0$$

if $n \neq n'$, in which case the systems (2.10) and (2.11) become, respectively

$$\frac{d\omega_n}{dt} = -\frac{1}{\varepsilon_n I_{nn}} \int_S F\left(\sum_{n'=1}^{N} \omega_{n'}, \Psi_{n'}\right) \Psi_n dS \qquad (2.12)$$

$$\text{for } n = 1,2,\ldots,N$$

and

$$\omega_n(0) = \frac{1}{I_{nn}} \int_S \omega(\vec{r},0)\, \Psi_n dS \qquad (2.13)$$

$$\text{for } n = 1,2,\ldots,N.$$

In practice different numerical methods are often combined in numerical models. We have already mentioned that a discrete representation in time is always used when a series expansion method is used in space. It is possible also to use different representations in the three space directions. In several models for example a discrete representation in the vertical direction is combined with a representation in terms of series expansions in the horizontal directions. In this case the procedure described above to obtain the space truncated equations is modified slightly. Before introducing the approximations of the horizontal fields the discretization in the vertical may be carried out by applying the model equations and integrals by finite difference quotients and quadrature formulae. The procedure described above will then apply to the resulting equations as these will be of the form (2.1). The only change is that each of the dependent variables in this case in independent of the vertical coordinate and that the domain S is two-dimensional instead of three-dimensional.

As mentioned above, the spectral method and the finite element method may be based on the same basic principles. The two methods differ, however, with respect to the choice of expansion functions. In the finite element method piece-wise - continuous functions of a compact support are used, i.e. functions each of which are different from zero only in a limited part of the region. In the spectral method on the other hand, one uses non-local continuous functions which are usually a subset of a complete system of orthogonal functions. The name "the spectral method" is due to the fact that the set of expansion coefficients of a certain variable are referred to as the spectrum of that variable.

In atmospheric models the spectral method has so far been used almost exclusively for large scale global or hemispheric numerical integrations and the expansion functions used in the representation of the horizontal fields have been surface spherical harmonics, although Hough functions (*Flattery*, 1970), (*Kasahara*, 1977; 1978) and trigonometric functions (*Orzag*, 1974) have also been proposed. The spectral representation in the horizontal direction has usually been combined with a discrete representation in the vertical direction, although a combination with a spectral representation (*Machenhauer and Daley*, 1972; 1974) as well as with a finite element representation (*Staniforth and Daley*, 1977) has also been considered.

3. BASIC PROPERTIES

3.1 Introduction

In this section we shall apply the spectral method to various simplified forms of the advection equation, describing one-dimensional advection. We shall first consider the simplest linear form of the advection equation and then proceed to more complex nonlinear equations. We have chosen to consider the advection equation basically because of its simplicity, but also because the advection process is a most important part of the atmospheric governing equations.

3.2 The linear advection equation

3.2.1 The analytical solution

The linear equation may be written

$$\frac{\partial u}{\partial t} + c\,\frac{\partial u}{\partial x} = 0 \; ; \qquad c = \text{constant}. \tag{3.1}$$

Here u(x,t) is the dependent variable, which we shall think of as the eastward velocity component at a certain latitude circle with length L. The independent variables are: x the distance along the latitude circle and the time t. For our purpose it is convenient to use the longitude $\lambda = (2\pi/L)x$ as independent variable instead of x, and to introduce the angular velocities $\omega = (2\pi/L)u$ and $\lambda = (2\pi/L)c$. Doing so (3.1) becomes

$$\frac{\partial \omega}{\partial t} + \gamma\,\frac{\partial \omega}{\partial \lambda} = 0 \; ; \qquad \gamma = \text{constant}, \tag{3.2}$$

which corresponds to (2.3) with $\mathcal{L}$ being the identity operator.

Clearly $\omega(\lambda,t)$ is a periodic function with period 2π, i.e.

$$\omega(\lambda,t) = \omega(\lambda + 2\pi p, t), \tag{3.3}$$

for all t and all integer p. Corresponding to (2.4) the initial condition is supposed to be given by

$$\omega(\lambda,0) = f(\lambda) \tag{3.4}.$$

It seems reasonable to assume the following properties of the true solution to (3.2). Firstly, it must be a single valued continuous real function of the independent variable, and secondly, the derivative $\partial\omega/\partial\lambda$ that appears in the differential equation must be defined everywhere (and consequently be continuous). Except perhaps for the assumption of no discontinuity points, these assumptions are justified as we are interested in physically relevant solutions only. With the above stated assumptions satisfied initially, that is for $\omega(\lambda,0) = f(\lambda)$ the general solution to (3.2) is

$$\omega(\lambda,t) = f(\lambda - \gamma t) \tag{3.5}$$

which satisfies the assumptions for all $t \geq 0$.

3.2.2 Choice of expansion functions

We shall consider the numerical solution to (3.2) obtained by the spectral method. A natural choice of expansion functions, $\Psi_n(\lambda)$, in this case is the trigonometric functions

$$\Psi_n(\lambda) = \begin{cases} \cos\left(\frac{n-1}{2}\lambda\right) & \text{for } n = 1,3,\ldots \\ \sin\left(\frac{n}{2}\lambda\right) & \text{for } n = 2,4,\ldots \end{cases}$$

It is well known that these functions form a complete system of orthogonal functions and that a wide class of functions can be represented by infinite Fourier series, which converge rapidly for sufficiently smooth functions. Furthermore, each of the functions is periodic with the period 2π, so that they satisfy the given boundary condition (3.3), and also they behave very simply under various operations of analysis, notably differentiation. Corresponding to (2.5) we seek an approximate solution of the form of the truncated Fourier series

$$\hat{\omega}(\lambda,t) = \frac{\omega_0^c(t)}{2} + \sum_{m=1}^{M} (\omega_m^c(t)\cos m\lambda + \omega_m^s(t)\sin m\lambda), \tag{3.6}$$

where for each Fourier component

$$(\omega_m^c(t) \cos m\lambda + \omega_m^s(t) \sin m\lambda) \ , \tag{3.7}$$

m is the zonal wavenumber, i.e. the number of waves along the latitude circle, and where M is the maximum wavenumber retained in the expansion. The number of time dependent expansion coefficients $\omega_m^c(t)$ and $\omega_m^s(t)$ in (3.7) is seen to be $N = 2M+1$. Introducing the complex functions $e^{im\lambda}$ (3.6) may be written as

$$\hat{\omega}(\lambda,t) = \sum_{m=-M}^{M} \omega_m (t) \, e^{im\lambda} \ , \tag{3.8}$$

where the complex coefficients for $m \geq 0$ are given by

$$\omega_m(t) = \frac{1}{2} (\omega_m^c(t) - i \, \omega_m^s(t)) \ , \tag{3.9}$$

defining $\omega_0^s \equiv 0$. The coefficients for negative and positive values of m are related by

$$\omega_{-m}(t) = (\omega_m(t))^* \tag{3.10}$$

with the asterisks denoting the complex conjugate. This last relation follows from the fact that $\hat{\omega}$ is a real function. We note that $\hat{\omega}$ is completely specified if the complex coefficients $\omega_m(t)$ are given for $0 \leq m \leq M$.

For the complex trigonometric functions we have the following orthogonality relation

$$\frac{1}{2\pi} \int_0^{2\pi} e^{im\lambda} \, e^{im'\lambda} d\lambda = \begin{cases} 1 & \text{for } m' = -m \\ 0 & \text{for } m' \neq -m \end{cases} \tag{3.11}$$

giving the following expression for the expansion coefficients in (3.8):

$$\omega_m(t) = \frac{1}{2\pi} \int_0^{2\pi} \hat{\omega} \, (\lambda,t) e^{-im\lambda} \, d\lambda \ . \tag{3.12}$$

3.2.3 The solution to the space truncated system

When using the spectral method the space truncated system, corresponding to (2.12), is generally called the truncated spectral equations. For the linear advection equation these equations are given below in (3.14) which is obtained as follows:

When (3.8) is substituted into (3.2) we immediately have

$$\sum_{m=-M}^{M} \left(\frac{d\omega_m}{dt} + im\gamma\, \omega_m \right) e^{im\lambda} = 0. \qquad (3.13)$$

As the expansion functions are linearly independent this equation is exactly satisfied if, and only if,

$$\frac{d\omega_m}{dt} = - im\gamma\omega_m \quad \text{for } -M \leq m \leq M. \qquad (3.14)$$

This is a system of 2 M + 1 complex equations, but due to the relation (3.10) it suffices to consider the equations for $0 \leq m \leq M$ only. We note that when deriving the truncated spectral equations for the linear equation considered no minimizing of a residue is needed, simply because the truncated series (3.8) exactly satisfies the equation. The reason is, of course, that the complex expansion functions are eigensolutions to the space differential operator $\partial/\partial\lambda$ involved in (3.2). As the only difference between the spectral method and the pseudo-spectral method is the way the residue is minimized we see that for the linear equation considered the two methods become identical. We note furthermore that each of the spectral equations can be integrated exactly in time if initial values of ω_m are given. The result is

$$\omega_m(t) = \omega_m(0)\, e^{-im\gamma t}. \qquad (3.15)$$

According to our assumptions f (λ) in (3.4) belongs to the class of functions, for which the corresponding Fourier series can be determined. That is,

$$f(\lambda) = \sum_{m=-\infty}^{\infty} a_m\, e^{im\lambda}. \qquad (3.16)$$

The proper initial values of ω_m, corresponding to (2.13), can therefore be obtained by computing the Fourier coefficients a_m of $f(\lambda)$

$$f(\lambda) \qquad a_m = \frac{1}{2\pi} \int_0^{2\pi} f(\lambda)\, e^{-im\lambda}\, d\lambda \qquad (3.17)$$

and using $\omega_m(0) = a_m$ for $0 \leq m \leq M$.

Substituting (3.15) into (3.8) we get the solution

$$\hat{\omega}(\lambda,t) = \sum_{m=-M}^{M} \omega_m(0)\, e^{im(\lambda - \gamma t)}\,. \qquad (3.18)$$

3.2.4 Convergence and consistency

It is obvious that if f (λ) can be represented exactly by a truncated Fourier series with maximum wavenumber equal to M (that is if $a_m = 0$ for $m > M$) then (3.18) is the exact solution. If this is not the case then (3.18) is only an approximate solution. Writing this approximate solution as

$$\hat{\omega}(\lambda,t) = f_M(\lambda-\gamma t)\,,$$

where

$$f_M(\lambda) \equiv \hat{\omega}(\lambda,0) = \sum_{m=-M}^{M} \omega_m(0)\, e^{im\lambda}$$

and using the fact that the exact solution is given by (3.5), the error function $\epsilon(\lambda,t) = \omega(\lambda,t) - \hat{\omega}(\lambda,t)$ may be written as

$$\epsilon(\lambda,t) = f(\lambda-\gamma t) - f_M(\lambda-\gamma t) \equiv \epsilon'(\lambda')\,,$$

where $\lambda' = \lambda-\gamma t$. thus, ϵ is independent of time in a coordinate system moving with the constant angular velocity γ. It is therefore never larger than the error we commit by approximating the initial function, $f(\lambda)$, by its Fourier series truncated at wavenumber M. Therefore, if the Fourier series of $f(\lambda)$ converges to $f(\lambda)$ then the approximate solution converges towards the exact solution, when M

approaches infinity. With the assumptions stated in subsection 3.2.1 satisfied for $f(\lambda)$ we know in fact that its Fourier series (3.16) does converge absolutely and uniformly.

The rate of convergence depends, of course, on $f(\lambda)$. Generally, the "smoother" the function, the faster the convergence.

According to the properties of the exact solution $\omega(\lambda,t)$ it may be represented by an infinite Fourier series

$$\omega(\lambda,t) = \sum_{m=-\infty}^{\infty} \tilde{\omega}_m(t)\, e^{im\lambda} , \tag{3.22}$$

which when substituted into (3.8) gives the system

$$\frac{d\tilde{\omega}_m}{dt} + im\gamma\tilde{\omega}_m = 0 \qquad \text{for } -\infty \leq m \leq \infty . \tag{3.25}$$

This infinite system of spectral equations is exactly equivalent to the differential equation (3.2). Comparing (3.25) with (3.14) we see that if $\omega_m = \tilde{\omega}_m$ the truncated system is consistent in the sense that (3.14) approaches (3.25) as M approaches infinity.

The convergence of $\tilde{\omega}$ to ω and the consistency of the truncated spectral equations rely on the assumption that $\omega = \tilde{\omega}_m$. This is the case if $f(\lambda)$ is given analytically as we have supposed above and if it satisfies the assumptions stated in subsection 3.2.1, so that the initial values can be determined exactly from (3.17). When the method is applied in practice, $f(\lambda)$ is usually not given analytically but determined from some analysis of observations and in actual practice the values will usually be available in some grid points λ_j. Let us suppose that K grid point values are given at the points $\lambda_j = (2\pi/K)j$ for $j = 1,2,\ldots, K$, where $K \geq 2M+1$. We may then get approximate values, a'_m of the complex coefficients by approximating the integral in (3.17) by the trapezoidal quadrature formula.

$$\frac{1}{2\pi}\int_0^{2\pi} g(\lambda)d\lambda \sim \frac{1}{K}\sum_{j=1}^{K} g(\lambda_j) . \tag{3.26}$$

This quadrature formula is exact if g (λ) is a truncated trigonometric series with maximum wavenumber M' = K -1 (e.g. *Krylov*, 1962). Using this quadrature we get instead of (3.17)

$$a'_m = \frac{1}{K} \sum_{j=1}^{K} f(\lambda_j)\, e^{-im\lambda_j} . \tag{3.27}$$

If f(λ) is a truncated trigonometric series with maximum wavenumber smaller than or equal to K-1-M then the values obtained by (3.27) for $|m| \leq M$ are equal to the exact values of a_m. If however, this is not the case then the small scale waves with wavenumbers larger than K-1-M are aliased on the large scale waves retained in the truncated spectral representation. By substituting the Fourier series (3.16) into (3.27) we get the relation

$$a'_m = \sum_{q=-\infty}^{\infty} a_{m+qK} \tag{3.28}$$

In the above derivation we have used the relationship that

$$e^{im\lambda_j} = e^{i(m+qK)\lambda_j}$$

for any integer q, and that

$$\frac{1}{K} \sum_{j=1}^{K} e^{im\lambda_j} e^{im'\lambda_j} = \begin{cases} 1 & \text{for } m = -m' \\ 0 & \text{for } m \neq -m' \end{cases} \tag{3.29}$$

when $|m + m'| \leq K-1$, which follows from (3.11) and the exactness property of the trapezoidal quadrature formulae mentioned above. Now according to our general assumptions about f(λ) we have $|a_m| \to 0$ for $m \to \infty$. Therefore the aliased contributions to a'_m (that is the contributions for $q \neq 0$ in the expression (3.28)) can be reduced as much as desired by increasing the value of K. That is, by increasing the number of points used in (3.27).

3.2.5 The equivalent grid point method

When using the spectral method we obtain an approximate solution in the form (3.8). This truncated Fourier series may be considered as an interpolating function fitting exactly the values of $\tilde{\omega}$ at the 2M + 1 points

$$\lambda_j = j(\Delta\lambda)_e, \quad j = 1,2,\ldots,2M+1,$$

where

$$(\Delta\lambda)_e = \frac{2\pi}{2M+1} . \tag{3.30}$$

We note that the relation between the 2M+1 grid point values $\hat{\omega}(\lambda_j,t)$ and the 2M+1 real coefficients determined by the coefficients $\omega_m(t)$ in (3.8) is unique. This follows from the fact that when the coefficients are given then by definition the grid point values are determined by

$$\hat{\omega}(\lambda_j,t) = \sum_{m=-M}^{M} \omega_m(t)\, e^{im\lambda_j}; \quad j = 1,2,\ldots,2M+1 \tag{3.31}$$

and when the grid point values are given the coefficients are determined uniquely by

$$\omega_m(t) = \frac{1}{2M+1} \sum_{j=1}^{2M+1} \hat{\omega}(\lambda_j,t)\, e^{-im\lambda_j} ; \quad -M \leq m \leq M , \tag{3.32}$$

which follows from (3.31) and (3.29). We shall refer to the grid defined by $\lambda_j = j(\Delta\lambda)_e$, $j = 1,2,\ldots,2M+1$ as <u>the equivalent grid</u>.

In order to compare the spectral method with the grid point method let us now transform the truncated spectral equations (3.14) to an equivalent system of differential equations which determine the time variation of the grid point values in the equivalent grid. this is done by multiplying each of the equations in (3.14) by $e^{im\lambda j}$ and then adding the resulting equations. Using (3.31) the result may be written as

$$\frac{d}{dt}\left(\hat{\omega}(\lambda_j,t)\right) = -\gamma \sum_{m=-M}^{M} im\omega_m(t)\, e^{im\lambda_j} .$$

	1	2	3	4	5	6	7	8
PS	1.006	-512	.351	-.274	.232	-.207	.192	-.186
2	.500	-	-	-	-	-	-	-
4	.667	-.083	-	-	-	-	-	-
6	.750	-.150	.017	-	-	-	-	-
8	.800	-.200	.038	-.004	-	-	-	-
10	.833	-.238	.060	-.010	.001	-	-	-
12	.857	-.268	.079	-.018	.003	-.000	-	-
14	.875	-.292	.097	-.027	.005	-.001	.000	-
16	.889	-.311	.113	-.035	.009	-.001	.000	-.000

TABLE 1: Comparison of weights defining derivatives with 17 grid points in a periodic domain. The weights have been multiplied by the grid length. The leftmost column indicates either the pseudo-spectral approximation (PS) or the order of the centred finite difference. The uppermost row is the number of grid lengths away from any central point of concern.

By substituting $\omega_m(t)$ given by (3.32) it may be shown (see *Machenhauer*, 1979) after some algebra that the spectral method when applied to the linear equation is equivalent to the application of the grid point method using the equivalent grid and a centered finite difference approximation for the derivative with respect to λ. This difference approximation is

$$\left(\frac{\partial \omega}{\partial \lambda}\right)_{\lambda=\lambda_j} \sim \sum_{k=1}^{M} C_k \left(\hat{\omega}(\lambda_{j+k},t) - \hat{\omega}(\lambda_{j-k},t)\right)$$

where $C_k = (-1)^{k+1}/2\sin(\pi k/2M+1)$.

It is determined by the use of a trigonometric series truncated at wavenumber M as an interpolating function, and is seen to involve all 2M neighbour points in the grid. The coefficients C_k are tabulated in Table 1 for the case M=8. This difference approximation may be considered to be of infinite order of accuracy since the truncation error goes to zero faster than any finite power of $(\Delta\lambda)_e$ if ω is supposed to be infinitely differentiable (*see Machenhauer*, 1979).

3.2.6 Discretization in time

Instead of using the exact solution (3.15) to the truncated spectral equation (3.14) a numerical integration in time may be carried out. For example when using the leapfrog scheme we obtain

$$\omega_m^{\tau+1} = \omega_m^{\tau-1} - i2m\gamma\Delta t\ \omega_m^{\tau} \ ; \quad -M \leq m \leq M \tag{3.35}$$

Here ω_m^{τ} is the approximate value of $\omega_m(t)$ at $t=\tau\Delta t$. We have already discussed how initial values can be determined and of course the values ω_m^{1} at $t=\Delta t$ must be determined from these values by some other time differencing scheme. For stability of the leapfrog scheme it is required that the condition

$$|m\gamma\Delta t| < 1$$

be satisfied for any admissible m. Since the maximum value of m in the truncated system of spectral equations is M we obtain the stability condition

$$|\gamma| M\Delta t \leq 1 \ . \tag{3.37}$$

In order to compare this criterion with those obtained for the grid point method using different finite difference approximations let us introduce $(\Delta\lambda)_e$, the grid interval in the equivalent grid defined by (3.30). The criterion (3.37) may then be written as

$$|\gamma| \left(\frac{\pi}{(\Delta\lambda)_e} - \frac{1}{2}\right)\Delta t < 1$$

or

$$\frac{|\gamma|\Delta t}{(\Delta\lambda)_e} < \frac{1}{\pi\left(1-\frac{1}{2M+1}\right)} \tag{3.38}$$

The corresponding stability criterion for the grid point method using second order centered difference approximation is

$$|\gamma|\frac{\Delta t}{\Delta\lambda} \leq 1 .$$

Similarly, linear stability of centered difference approximations with spatial error of order $(\Delta\lambda)^n$, for $n>2$ may be shown to require

$$|\gamma|\frac{\Delta t}{\Delta\lambda} \leq \kappa_n ,$$

where the first few values of κ_n are $\kappa_4=0.73$, $\kappa_6=0.63$ and $\kappa_8=0.59$. As $n\to\infty$ the value κ_n approaches $1/\pi$, which is in fact approximately the stability limit found in (3.38) for the spectral method.

The most unstable wave in the spectral system (3.35) is the wave with $m=M$, which has a wavelength equal to

$$2(\Delta\lambda)_e\left(1 - \frac{1}{2M+1}\right)^{-1} .$$

For second order centered difference approximation on the other hand, the most unstable wave with a wavelength equal to 4 grid intervals. When centered difference approximations of higher order are used the wavelength of the most unstable wave is reduced and when the order n approaches infinity it approaches 2 grid intervals, which is approximately the wavelength of the most unstable wave in the spectral system.

3.2.7 Concluding remarks

Before proceeding to the nonlinear advection equation we shall summarise and comment on the main results obtained for the linear equation.

When errors due to discretization in time and initial aliasing can be ignored the spectral method gives the exact solution for all wave components retained in the truncated Fourier series. This implies in particular that the phase speed of all retained spectral components is represented exactly, except for time truncation errors, whereas the usual finite difference schemes suffer from phase speed errors

due to space truncation which increases with decreasing wavelength. This implies that when using the spectral method no computational dispersion, such as that observed with the grid point method, results from the space truncation. We have furthermore seen that the truncated spectral equations are consistent with the differential equation and that for sufficiently smooth initial conditions the numerical solution converges uniformly to the exact solution.

In the spectral method an approximate value of the space derivative is determined, which may be considered as equivalent to that of the grid point method with a centered finite difference approximation of infinite order of accuracy. The properties of schemes obtained from the truncated spectral equations by introducing various time difference approximations can be inferred from results obtained for the oscillation equation. We have seen in particular that for the leapfrog scheme results are obtained which are consistent with the fact that the spectral method corresponds to a centered difference method of infinite order of spatial accuracy.

3.3 The nonlinear advection equation

3.3.1 Properties of the true solution

Choosing again as dependent variable the angular velocity $\omega(\lambda,t)$ the nonlinear advection equation may be written

$$\frac{\partial \omega}{\partial t} = -\omega \frac{\partial \omega}{\partial \lambda} , \tag{3.39}$$

where $\omega(\lambda,t)$ is supposed to be periodic with period 2π, i.e. satisfies (3.3), and where the initial condition is given by (3.4). We note that (3.39) is of the form (2.3) with $\mathcal{L}$ being the identity operator.

The solution to (3.39) satisfying the initial condition (3.4) is

$$\omega(\lambda,t) = f(\lambda - \omega(\lambda,t)t) \tag{3.40}$$

which takes constant values $\omega=\omega(\lambda_0,0)=f(\lambda_0)$ in the λ,t - plane along the characteristics, the lines

$$\lambda = \omega(\lambda_o,0) \; t+\lambda_o \; . \tag{3.41}$$

With the same justifications as those given in subsection 3.2.1 we require ω at a certain time to be a single valued continuous real function with a derivative with respect to λ defined everywhere. For the linear equation, considered in the previous subsection it is sufficient that ω initially satisfies these conditions, since the solution in this case propagates along the λ-axis without change of form with the constant angular velocity γ, or in other words because all the characteristics are straight lines with the same slope γ. For the nonlinear advection equation considered here this is generally not the case. The characteristics (3.14) are straight lines too but (expect for the special case $\omega(\lambda,0)=f(\lambda)=$constant) they have different slopes. The shape of ω is therefore changing as t is increasing and sooner or later two or more characteristics will cross. At the breakdown time $t=t_B$, when this happens for the first time, $\partial\omega/\partial\lambda$ becomes infinite at the crossing point and after the breakdown time, the solution becomes multivalued in the neighbourhood of this point. Physically the significance of the solution (3.40) is therefore limited to the time interval $0\leq t\leq t_B$. We shall consequently only consider the solution in this time interval and furthermore we shall assume that the initial conditions are sufficiently smooth to ensure the above mentioned properties of ω during the whole time interval.

As a simple example, which illustrates the breakdown of the true solution, consider the solution obtained by *Platzman* (1964) for the special case $\omega(\lambda,0)=f(\lambda)=-\sin\lambda$ shown in Fig. 1. The right panel of the figure is a λ,t - diagram which shows a few typical characteristics (3.14). Also shown is the envelope of the "cusp region" inside which the solution is triple valued (three characteristics through each point). It is seen that in this case $t_B=1$. The left panel of Fig. 1 shows $\omega(\lambda,t)$ at selected times. We shall return to this case in subsection 3.3.5 where the exact solution will be compared with numerical solutions obtained by the spectral method in the time interval $0\leq t\leq t_B$.

For later reference we note the following general properties of the solution to (3.39) valid for $0\leq t\leq t_B$, namely that the moments $\overline{\omega^p}$ are invariants or that

$$\frac{d}{dt}\ \overline{\omega^p} = 0 \qquad (3.42)$$

for p equal to any natural number, where the bar indicates the mean value defined by

$$\overline{(\ )} = \frac{1}{2\pi}\int_0^{2\pi}(\ )\,d\lambda\,. \qquad (3.43)$$

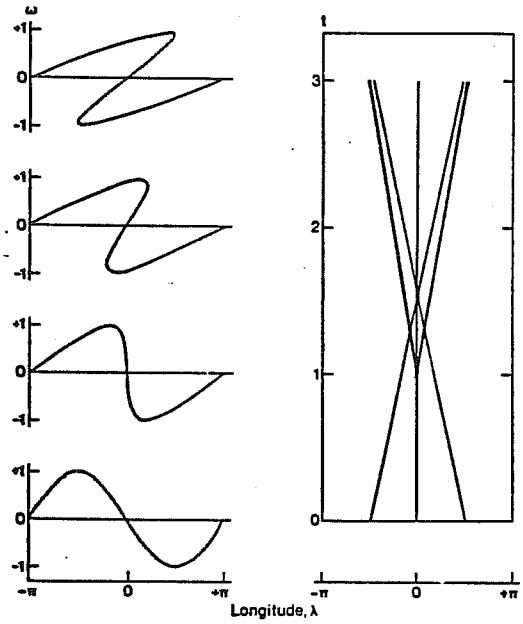

FIG. 1

Left panel : profiles of ω as a function of λ for t=0, t=1, t=2 and t=3.
Right panel:λ,t - diagram showing characteristics ω=0 and ω=±1.
Heavy curve with cusp at t=1 is envelope of the region inside which the solution is triple valued.
(After Platzman (1964)).

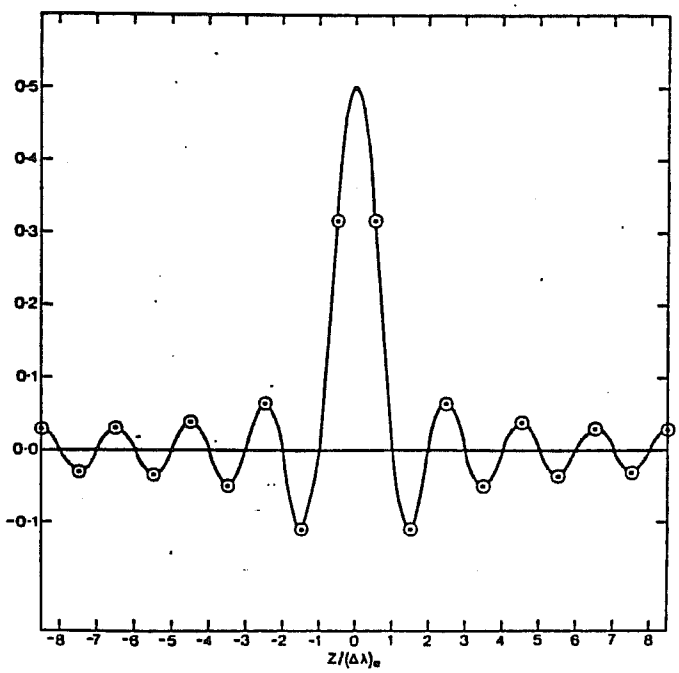

FIG. 2

The weight function $W^{(N)}(Z)/2N$ for N=17 (see eq. (3.67)); the abscissa is marked in units of $Z/(\Delta\lambda)_e$.

This result is obtained as follows: After multiplication by $p\omega^{p-1}$, equation (3.39) may be written

$$\frac{\partial}{\partial t}\,\omega^{p} + \frac{p}{p+1}\,\frac{\partial}{\partial \lambda}\,\omega^{p+1} = 0 .$$

As ω is periodic with period 2π, application of the operator (3.43) gives (3.42).

Two moments in particular are of interest here: namely the first and second moments which are proportional to the mean momentum and to the mean kinetic energy, respectively.

3.3.2 The space and time truncated system

Choosing again trigonometric basic functions we seek an approximate solution of the form (3.6) or (3.8). That is

$$\hat{\omega}(\lambda,t) = \sum_{m=-M}^{M} \omega_m(t)\, e^{im\lambda} . \tag{3.44}$$

As noted before, this form satisfies the boundary condition (3.3), however, it is easily shown by substitution that in the general case, when $\omega_m \neq 0$ for all admissible values of m, this form does not satisfy the nonlinear equation exactly. For the right-hand side of (3.39) we get

$$F(\hat{\omega}) = -\hat{\omega}\,\frac{\partial \hat{\omega}}{\partial \lambda} = \sum_{m=-2M}^{2M} F_m\, e^{im\lambda}, \tag{3.45}$$

where

$$F_m = \frac{1}{2\pi}\int_0^{2\pi} \left(-\sum_{m_1=-M}^{M} \omega_{m1}\, e^{im_1\lambda}\right)\left(\sum_{m_2=-M}^{M} im_2\, \omega_{m2}\, e^{im_2\lambda}\right) e^{-im\lambda}\, d\lambda \tag{3.46}$$

or

$$F_m = -i \sum_{m_1=m-M}^{M} (m-m_1)\, \omega_{m_1}\, \omega_{m-m_1} \qquad \text{for } m \geq 0. \tag{3.47}$$

Here the expression (3.47) is obtained from (3.46) by carrying out the multiplication of the series in the integrand and by using the orthogonality condition (3.11). Note that (3.47) is valid only for $m \geq 0$. For the left-hand side of (3.39) we get

$$\frac{\partial \hat{\omega}}{\partial t} = \sum_{m=-M}^{M} \frac{d\omega_m}{dt} e^{im\lambda} . \tag{3.48}$$

Thus the substitution of (3.44) in (3.39) gives truncated Fourier series on both sides, but the series are truncated at different wavenumbers, and as the trigonometric functions are linearly independent, we will, regardless of how the values of the coefficients $d\omega/dt$ are determined, generally get a residue

$$R(\hat{\omega}) = \frac{\partial \hat{\omega}}{\partial t} + \hat{\omega} \frac{\partial \hat{\omega}}{\partial \lambda} , \tag{3.49}$$

which is not identically zero for all λ.

Now, in accordance with the general description of the spectral method in section 2, we choose those values of $d\omega/dt$ which minimize the mean value of the residue. That is, the values determined by

$$\int_0^{2\pi} R(\hat{\omega}) \, e^{-im\lambda} \, d\lambda = 0 \qquad \text{for } -M \leq m \leq M , \tag{3.50}$$

which corresponds to the system (2.7). Using (3.49), (3.48), (3.45) and the orthogonality condition (3.11) we get from (3.50) the truncated spectral equations

$$\frac{d\omega_m}{dt} = F_m \quad ; \qquad -M \leq m \leq M , \tag{3.51}$$

which corresponds to (2.12) in the general case.

The minimised residue obtained by this procedure may be determined as follows. We multiply each of the equations in (3.51) by $e^{im\lambda}$, add the resulting equations and get

$$\frac{\partial \hat{\omega}}{\partial t} = \hat{F}(\hat{\omega}),$$

$$\hat{F}(\hat{\omega}) = \sum_{m=-M}^{M} F_m e^{im\lambda} . \qquad (3.52)$$

When this expression and the expression (3.45) are substituted in (3.49) we find

$$R(\hat{\omega}) = -\sum_{M<|m|\leq 2M} F_m e^{im\lambda} . \qquad (3.53)$$

We see that the approximate value $\partial\hat{\omega}/\partial t = \hat{F}(\hat{\omega})$ is obtained from the true value $(\partial\omega/\partial t)_{\omega=\hat{\omega}} = F(\hat{\omega})$ simply by neglecting the Fourier components F_m of the nonlinear term with wavenumbers larger than M. Thus, all Fourier components retained in the truncated representation are computed without any aliasing of smaller scale components outside the truncation. This is a basic property of the spectral method and as a consequence the type of nonlinear instability described by *Phillips* (1959) is prohibited in spectral models. The non-aliased truncation is a consequence of minimising the least square value of residue $R(\hat{\omega})$ and the choice of orthogonal expansion functions.

When using the spectral method the full consequence is taken of the fact that only a finite number of components is included in the truncated spectral representation. Within this limitation the best all over approximation in a least squares sense is determined by neglecting the tendencies of the components which cannot be represented.

A further property of the truncated spectral system is that the first and the second moments are invariants. We have seen that this is the case also for the exact equation, which in addition conserves higher moments. These properties of the truncated spectral equations, namely that $\overline{d\hat{\omega}/dt}=0$ and $\overline{d\hat{\omega}^2/dt}=0$ follows from the fact that

$$\overline{R(\hat{\omega})} = 0 \qquad (3.56)$$

and

$$\overline{\hat{\omega}\, R(\hat{\omega})} = 0 \,. \tag{3.57}$$

Note that (3.57) and consequently the conservation of $\tilde{\omega}^2$is a general property of methods built upon the Galerkin approximation (this result was obtained in equation (2.9)). The first moment $\tilde{\omega}$ is equal to the Fourier coefficient ω_0 so that according to (3.51) the conservation of this moment should imply that $F_0=0$. That this is the case may be verified directly from the expression (3.47).

Introducing the deviation, $\hat{\omega}'=\hat{\omega}-\omega_0$, from the mean angular velocity ω_0 the nonlinear term $F(\hat{\omega})$ may be split up in the following two contributions

$$F(\hat{\omega}) = -\omega_0 \frac{\partial \hat{\omega}'}{\partial \lambda} - \hat{\omega}' \frac{\partial \hat{\omega}'}{\partial \lambda}$$

It is easily seen that the linear term, $-\omega_0 \partial\hat{\omega}'/\partial\lambda$, does not contribute to the minimised residue $R(\hat{\omega})$ and thus, that the contributions to the phase velocities for all retained components from this linear term are computed exactly. Consequently, just as for the linear equation discussed in Subsection 3.2, a cause of computational dispersion is hereby eliminated.

The truncated spectral equations (3.51) are a system of first order nonlinear differential equations. This system is much more complicated than the system (3.14) obtained for the linear advection equation and, except for cases with very small values of M, it does not seem possible to find analytical solutions. Thus, a numerical integration in time must be carried out by means of some time differencing scheme. Choosing for instance the leapfrog scheme the numerical solution, after the first step, is determined by the system

$$\begin{cases} \omega_m^{(\tau+1)} = \omega_m^{(\tau-1)} + 2\Delta t\, F_m^{(\tau)} \quad \text{for} \begin{cases} \tau \geq 2 \\ 1 \leq m \leq M \end{cases} , \\ F_m^{\tau} = -\, i \sum_{m_1=m-M}^{M} (m-m_1)\, \omega_{m1}^{(\tau)}\, \omega_{m-m_1}^{(\tau)} \,. \end{cases} \tag{3.58a}$$

As usual $\omega_m^{(\tau)}$ to be used in (3.58a) may for instance be determined by two initial time steps: a forward one of $\Delta t/2$ and a centered one of Δt each from time zero. That is by

$$\left\{\begin{array}{lll} \omega_m^{(\frac{1}{2})} & = \omega_m^{(0)} & + \frac{\Delta t}{2} F_m^{(0)} \\ \omega_m^{(1)} & = \omega_m^{(0)} & + \Delta t\, F_m^{(\frac{1}{2})} \end{array}\right\} \quad \text{for} \quad 1 \leq m \leq M \,. \qquad (3.58b)$$

In order to obtain computational stability a conservative estimate of Δt may be obtained from (3.37) by using γ equal to the maximum value of $|\hat{\omega}(\lambda,0)|$ (which for the true solution at least is conserved during the integration).

The conservation of the second moment or the mean kinetic energy should ensure absolute computational stability, since the magnitude of the solution is necessarily bounded. Actually the mean kinetic energy is only quasi-conserved if a time discretization is introduced. Nevertheless, the time truncation errors are usually small and in any case the non-aliased truncation should still prevent the Phillips-type of non-linear instability.

3.3.3 Consistency and convergence

If we assume initial conditions which give smooth solutions (for $0 \leq t \leq t_B$) then we obtain that the truncated system (3.51) is consistent in the sense that for M approaching infinity it converges to a system which is equivalent to the differential equation.

Concerning convergence of the numerical solution to the true solution it does not seem possible, even for the simple nonlinear advection, to establish error bounds from which such a convergence can formally be proven. this is, however, also the present situation for other numerical methods. For the nonlinear advection equation we have already seen that the mean velocity and the mean kinetic energy are conserved, when errors due to time discretization can be neglected. This, of course, puts bounds on the error. However, it seems not possible to obtain proof of convergence from these bounds. The lack of a formal proof does, however, not imply that the numerical solution does not converge to the true solution with increasing resolution. On the contrary, practical experience with cases where the true solution can be determined indicates such a convergence.

3.3.5 Comparison of a particular exact solution and corresponding numerical solutions

Following *Platzman* (1964) we shall in this subsection consider the solution to the nonlinear advection equation (3.39) in the special case

$$\omega(\lambda,0) = f(\lambda) = -\sin\lambda \ . \tag{3.73}$$

The general solution (3.40) becomes

$$\omega(\lambda,t) = -\sin(\lambda - \omega t) \tag{3.74}$$

which keeps $\omega = 0$ at all points where λ is an integral multiple of π. Therefore prior to the time of shock formation ($t<t_B = 1$), this solution has a well-defined Fourier sine-series representation:

$$\omega(\lambda,t) = \sum_{m=1}^{\infty} \tilde{\omega}_m^s(t) \sin m\lambda \ , \tag{3.75}$$

where

$$\tilde{\omega}_m^s(t) = \frac{1}{\pi} \int_{-\pi}^{\pi} \omega(\lambda,t) \sin m\lambda \, d\lambda \ . \tag{3.76}$$

It is remarkable, and one of the main points of the paper by *Platzman* (1964), that in spite of the implicit nature of the solution (3.74), the coefficients (3.76) of the exact solution can be evaluated explicitly.

We are going to compare the exact solution with numerical solutions determined by the spectral method using different truncations and the leapfrog time differencing scheme. These numerical solutions are determined by the system (3.58). The initial condition (3.74) implies that $\omega_m(0) = 0$ for $m \neq 1$ and $\omega_1(0) = i/2$. Results from integrations with three different truncations, M = 5, M = 20, and M = 60, will be presented. In all cases a time step $\Delta t = 1/100$ was used.

Considering at first the exact solution, the solid lines in Fig. 3 show the values of $-\tilde{\omega}_m^s(t)$ for $0 \leq t \leq 1$. Fig. 3a shows results for m = 1(1) 5 and Fig. 3b shows (on expanded scale) results for m = 6(1)10,15,20 (10) 60. All coefficients are zero initially with exception of $\tilde{\omega}_1^s(0) = -1$. As t increases

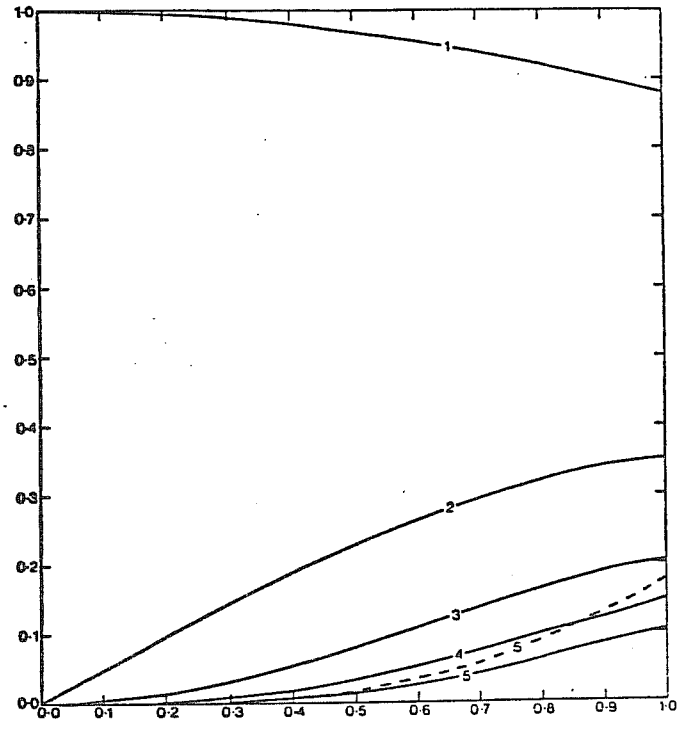

Figure 3a

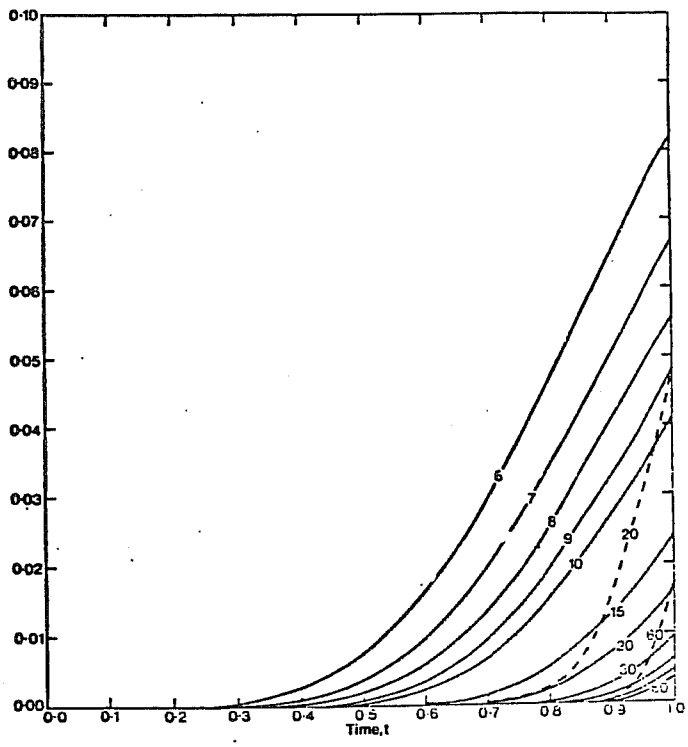

Figure 3b

FIG. 3

Solid curves : $-\tilde{\omega}_m^s(t)$ computed from (3.78); in (a) for m=1(1)5 and in (b) for m=6(1)10,15,20(10) 60.
Broken curves: $-\omega_m^s(t)$ computed from (3.80); in (a) for m=M=5 and in (b) for m=M=20 and m=M=60.
(Note that ordinate scales of (a) and (b) differ by a factor of 10.)

from zero, $|\tilde{\omega}_1^s(t)|$ gradually declines as energy cascades through the spectrum. In each of the other harmonics the energy increases monotonically throughout the range $0 \leq t \leq 1$.

As shown in subsection 3.3.1 the second moment $\overline{(\omega(\lambda,t))^2}$ is an invariant of the differential equation (3.39). $\overline{(\omega(\lambda,t))^2}$ is proportional to the mean kinetic energy and it is easily shown that in the case considered

$$\overline{(\omega(\lambda,t))^2} = \frac{1}{2} \sum_{m=1}^{\infty} K_m(t) = \frac{1}{2} .$$

$K_m(t)$ may therefore be considered as the contribution from wavenumber m to the total kinetic energy

$$K = \sum_{m=1}^{\infty} K_m(t) = 1 .$$

At $t = 1$, the limit of the "physical" range, the spectrum

$$K_m(t) = (\tilde{\omega}_m^s(t))^2$$

is shown by the solid lines in Fig. 4 for $m \leq 120$. 99.98 per cent of K is included in the part of the spectrum shown.

Due to the increasing slope of the solution at $\lambda = 0$ (see Fig. 1) the series (3.75) converges less and less rapidly as t approaches 1 and for $t = 1$ the convergence is rather slow due to the infinite slope of the exact solution at $\lambda = 0$. At $t = 1$, K_M is very nearly proportional to $m^{-8/3}$.

The mean square error of the numerical solution is

$$e(\tau\Delta t) = \overline{(\omega(\lambda,\tau\,\Delta\,t) - \hat{\omega}^{(\tau)}(\lambda))^2} .$$

This error may be split up into two contributions:

$$e(\tau\,\Delta\,t) = e_A(\tau\Delta t) + e_B(\tau\Delta t) ,$$

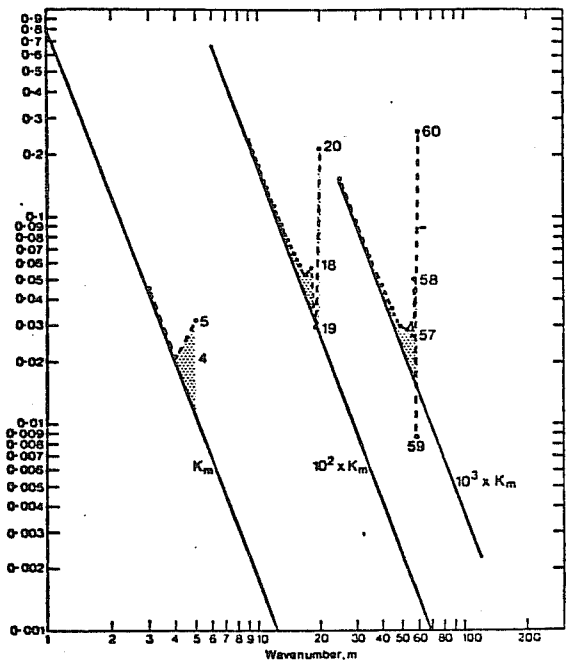

FIG. 4

The spectrum of kinetic energy at t=1. Solid curves show K_m and the broken curves show $\hat{K}_m$ for M=5, M=20 and M=60.

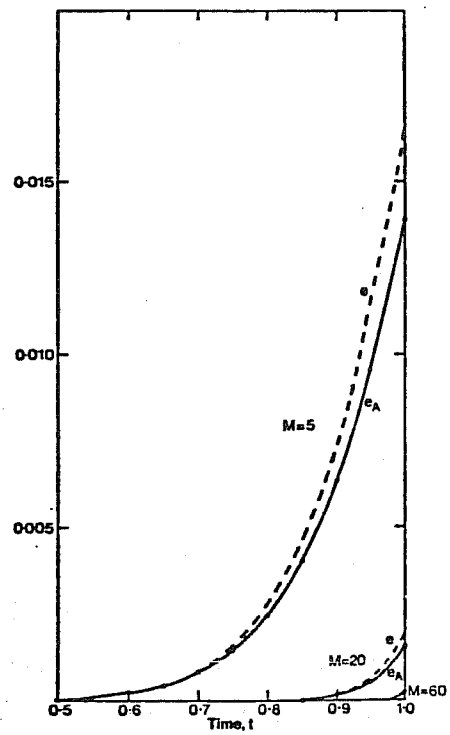

FIG. 5

The mean square error e and the contribution e_A(see text) for different truncations :M=5, M=20, and M=60.

e_A is the mean square error introduced by truncating the exact solution (3.75) and e_B is the error introduced by using the numerically determined coefficients $\omega_m^{s(\tau)}$ instead of ϖ_m^s $(\tau\Delta t)$ for $1 \leq m \leq M$.

It is obvious that e can never be smaller than e_A, which in the case considered must increase with time due to the energy cascade. The growth of e and e_A with time for the three different truncations is shown in Fig. 5. It is seen that the main contribution to e comes from e_A whereas the contribution from e_B is relatively small. Furthermore, at a certain time e decreases with increasing resolution which demonstrates that the numerical solution converges towards the exact solution.

Before $t = 0.5$ even the low solution with $M = 5$ deviates very little from the exact solution. In Fig. 6 the exact solution ω, the truncated exact solution ω_T and the numerical solution $\tilde{\omega}$ for the low resolution integration in the interval $-\pi \leq \lambda \leq 0$ and for $t = 0.2\ (0.2)1.0$ are shown. On the scale chosen in the figure, it is not possible to see any deviation between the three solutions at $t = 0.2$ and $t = 0.4$. At $t = 0.6$ a small deviation between ω and the solutions ω_T and $\tilde{\omega}$ can be seen, ant at $t = 0.8$ and in particular at $t = 1.0$ the differences between all three solutions can be seen clearly.

We have seen that the main contribution to the deviation between the numerical solution $\tilde{\omega}$ and the exact solution ω is due to lack of resolution, however, some deviation does develop between $\tilde{\omega}$ and ω_T. In order to illustrate how this deviation is distributed on the different wavenumbers m retained in the truncated representations, the values of $\hat{K}_m = (\omega_m^s)^2$ at $t = 1$ have been plotted on Fig. 4 for the three cases $M = 5,20$ and 60.

It was shown in Section 3.2.2 that the second moment $\tilde{\omega}^2$ is an invariant also for the truncated spectral equations. In the present numerical integrations we should therefore find that if round-off errors and time truncation can be neglected

$$K = \sum_{m=1}^{M} \hat{K}_m(t) = 1$$

during the whole integration. This was found to be the case in practice to a very high degree of precision. The difference between K_m and $\hat{K}_m$ is seen to be concentrated on the highest wavenumbers retained in the representation and generally $\hat{K}_m$ is larger than K_m. Especially, the value of the energy, $\hat{K}_m$, in the very last component with $m = M$ is seen to be predicted much too high. During the

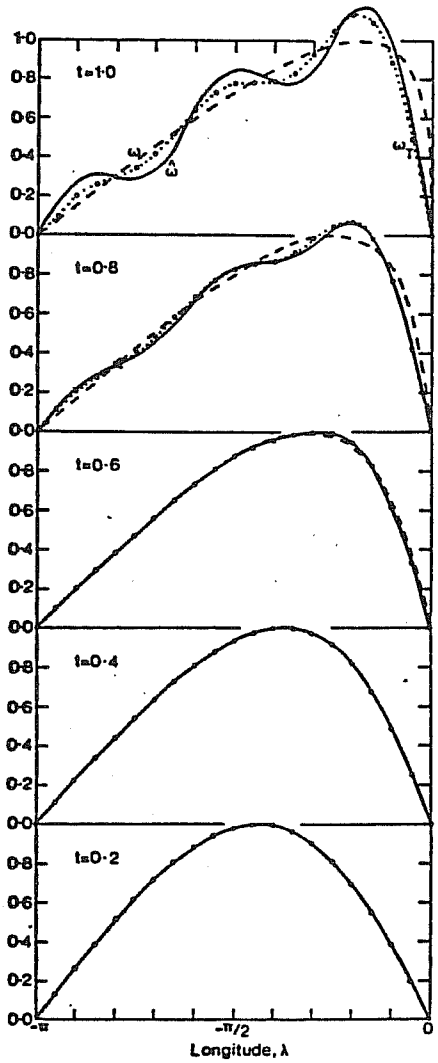

FIG. 6 The exact solution ω (dashed curves), the truncated exact solution ω_T (dotted curves), and the numerical solution $\hat{\omega}$ (solid curves) at selected t; ω_T and $\hat{\omega}$ are for M=5.

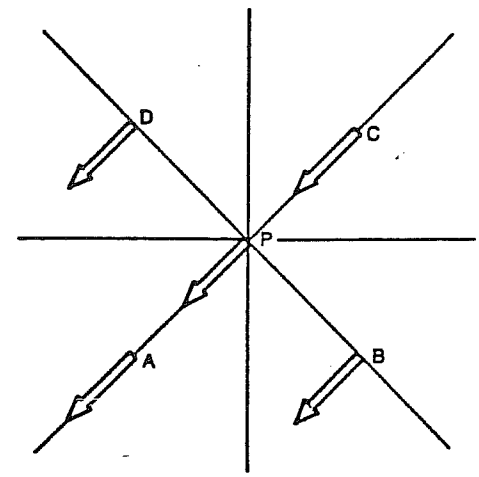

FIG. 7 The velocity vector at five points at and near the north pole P.

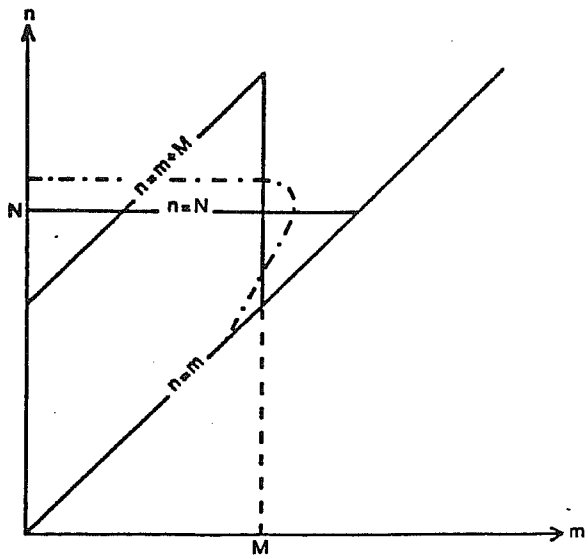

FIG. 9

Limits used in different types of truncation. The dot-dashed curve shows the approximate form of isopleths of kinetic energy, presented by Baer (1972).

course of the numerical integration energy is piling up in the shortest waves retained in the representation. Intuitively, we should expect this phenomenon, known as blocking, to occur in the present numerical integrations, as we are trying to simulate a cascade of energy towards higher wavenumbers using a truncated representation within which the total energy is conserved. In order to illustrate the development in time, we have plotted in Fig. 3 the value of $-\omega_m^{s(\tau)}$ (the absolute values of the very last component retained in the three numerical integrations). A comparison with the exact values $-\varpi_m^s$ shows that the significance of the blocking phenomenon decreases with increasing resolution and that it occurs at a later time in high resolution integrations.

Blocking is due to the neglect of interactions involving components outside the truncation limit and it seems likely, at least in the present example, that the effect of the neglected components could be parameterized by a simple scale selective dissipation of energy at the highest wavenumbers retained. thereby, the contribution e_B to the mean square error e could probably be reduced substantially.

Blocking does occur also in the global models to be considered in the following section and in these models a parameterization in terms of a scale selective dissipation are used in order to reduce the errors due to blocking.

4. MODELS IN SPHERICAL GEOMETRY

4.1 Historical introduction

The spectral method was introduced into meteorological modelling as early as 1954 by *Silberman* (1954), who considered the non-divergent barotropic vorticity equation in spherical geometry. During the following years studies of the method were performed (notably by *Kubota* , 1959, *Lorenz*, 1960, *Platzman*, 1960, *Kubota et al.*, 1961, *Baer and Platzman*, 1961, *Baer*, 1964 and *Ellsaesser*, 1966). These studies demonstrated several desirable properties of the spectral method, and the study of *Ellsaesser* (1966) even indicated that for a balanced barotropic model the spectral method could compete with the grid point method used at the U.S. National Meteorological Center at that time with respect to performance and efficiency. The spectral method seemed feasible at a low resolution for this simple model. It was, however, not considered to be a realistic alternative to the grid point method for high resolution integrations of complex non-adiabatic models. The reason for this was that the method used in the computation of the nonlinear terms in the equations involved storing of a large number of so-called interaction coefficients, the number of which increases very fast with increasing resolution. As this method involves a number of arithmetic operations per time step

approximately proportional to the number of interaction coefficients it could be foreseen that the computing time and storing space requirements would exceed all practical limits at high resolutions. Furthermore, it was not easy to see any practical solution to the problem of incorporating locally dependent physical processes, such as release of precipitation or a convective adjustment.

The interaction coefficient method survived unchallenged until *Robert* (1966) suggested the use of low-order non-orthogonal spectral functions based on elements of spherical harmonics. This approach eliminated the complexity of interaction coefficients at the expense of an orthogonalization procedure at each time step. Thus, the storage problem was eliminated. The bias of a very rapid increase in arithmetic operations with increasing resolution and the inclusion of locally independent physical processes remained, however, unsolved problems.

The situation was completely changed with the introduction of the transform method developed independently by *Eliasen et al.* (1970) and *Orszag* (1970). In this method no interaction coefficients are involved and the required storage as well as the number of arithmetic operations is reduced substantially. Furthermore, the method involves a stage in each time step where point values of the dependent variables are computed in an auxiliary grid in the physical space. As pointed out by *Eliasen et al.* (1970) this made a direct inclusion of locally dependent non-adiabatic effects possible, in a way similar to that used in grid point models. The transform method in a one-dimensional version was tested by *Eliasen et al.* (1970) for a hemispheric shallow water model (i.e. a single level primitive equations model). Subsequently *Bourke* (1972) and *Machenhauer and Rasmussen* (1972) tested the full two-dimensional transform method for the same model. The results were very encouraging. Even at relatively low resolution an order-of-magnitude improvement in efficiency was obtained compared to the interaction coefficient method, and as this factor increases rapidly with resolution, spectral models with much higher resolution seemed now feasible. Several groups started the development of complex global or hemispheric baroclinic models utilizing the transform method. Descriptions of these models and reports on the first experiments were published during the following years (*Machenhauer and Daley*, 1972 and 1974, *Bourke*, 1974, *Hoskins and Simmons*, 1975, *Daley et al.*, 1976, *Bourke et al.*, 1977, and in the report from the Symposium on Spectral Methods held in Copenhagen in 1974: *Bourke et al*, 1974, *Eliasen and Machenhauer*, 1974, *Daley et al.*, 1974, *Gordon and Stern*, 1974 and *Hoskins and Simmons*, 1974).

4.2 Choice of dependent variables and expansion functions

Let us consider the complete set of quasi-hydrostatic equations used in atmospheric models, and assume that a discretization in the vertical direction has already been carried out. The system of prognostic equations may then quite generally be written in the form (2.1), where the prognostic variables are functions only of geographical position and time.

As explained in Section 2 the spectral method is based on a representation of the variables in terms of a common set of expansion functions which are non-local continuous functions, defined over the whole region. In global spectral models all variables must therefore be defined everywhere on the sphere. Thus, we must avoid using vertical coordinates in which the coordinate surfaces intersect the lower boundary surface. As mentioned in Section 2 spherical harmonics are usually chosen as expansion functions and we shall only consider models in which these functions are used. One advantage of this choice is that the equations in spherical coordinates can be used directly without any mapping. The spherical harmonics will be defined below and we shall see that expansions in terms of these functions converge very fast for sufficiently smooth functions. For functions having dis-continuity points the series may still converge if the functions are otherwise smooth. The convergence will, however, be much slower, especially in the neighbourhood of such discontinuity points, where the Gibbs' phenomenon (*Courant and Hilbert*, 1953) may be observed. It seems therefore reasonable that the dependent variables are chosen in such a way that discontinuities are avoided, if possible. This is especially relevant when choosing the variables describing a horizontal velocity field $\vec{V}$. We may choose to describe the velocity field by either the fields of a stream function ψ and a velocity potential χ or by the fields of u and v, (the velocity components toward the east and the north, respectively). If we assume that $\vec{V}$ is continuous everywhere on the sphere, then this is the case for ψ and χ also, whereas u and v generally (if $\vec{V} \neq 0$ at the poles) are discontinuous at the poles. This is illustrated in Fig. 7, which shows the velocity vector at five points at and near the north pole P. When approaching P from A the component v approaches $-|\vec{V}_p|$, whereas the limit of v is $|\vec{V}_p|$ when approaching P from C. Thus v is discontinuous at the pole point. Similarly it is seen that u is discontinuous at P along the meridian BD. Along the two other meridians shown both u and v are discontinuous at P. Thus, if u and v were chosen as dependent variables to be represented by series of spherical harmonics, these series would generally converge very slowly and furthermore as any series of spherical harmonics is continuous everywhere, in particular at the poles, it is not possible to describe even the most simple continuous wind vector field, with a non-zero wind at a pole point, by the use of truncated series for u and v. It follows that when using the spectral method

with spherical harmonics as expansion functions ψ and χ are appropriate scalar variables to be used in representing the horizontal velocity field, whereas u and v are not. This can be achieved easily by using the differentiated forms of the equations of motion instead of the primitive equations (that is, the vorticity and divergence equations instead of the equations for the horizontal velocity components). We shall see later that this corresponds to the use of the primitive equations using special expansion series for u and v. For the time being we shall, however, assume that ψ and χ are chosen as variables and that the differentiated equations are used. We note that in this case and for these equations the operator $\mathcal{L}_i$ in (2.1) becomes equal to the spherical Laplacian.

For the partial differential model equations with given initial conditions we assume the existence of a true solution and that the true fields of prognostic variables for $t \geq 0$ are single valued continuous real functions with continuous derivative up to at least the second order over the entire sphere. If these assumptions are satisfied the true solution may be represented by infinite series of surface spherical harmonics which are absolutely and uniformly converging (*e.g. Courant and Hilbert*, 1953). Actually the series will converge pointwise under considerably weaker conditions (*e.g. Rectory*, 1969, *and Hobson*, 1955). Considering for instance the stream function ψ, the dependence upon the latitude ϕ and the longitude λ may be expressed by the series

$$\begin{aligned}\psi(\lambda,\phi,t) &= \tfrac{1}{2}\,\tilde{\psi}^{c}_{0}(\phi,t) \\ &\quad + \sum_{m=1}^{\infty}\left(\tilde{\psi}^{c}_{m}(\phi,t)\cos m\lambda + \tilde{\psi}^{s}_{m}(\phi,t)\sin m\lambda\right) \\ &= \tfrac{1}{2}\sum_{n=0}^{\infty}\tilde{\psi}^{c}_{0,n}(t)\,P_{0,n}(\phi) \\ &\quad + \sum_{m=1}^{\infty}\sum_{n=m}^{\infty}\left(\tilde{\psi}^{c}_{m,n}(t)\cos m\lambda + \tilde{\psi}^{s}_{m,n}(t)\sin m\lambda\right)P_{m,n}(\phi).\end{aligned} \tag{4.1}$$

Here the first series is a Fourier series at a certain latitude circle, as those used in Section 3. The second series is the expansion of ψ in terms of spherical harmonics.

The functions $P_{m,n}(\mu)$ denote the associated Legendre functions of the first kind of order m and degree n, which may be defined by

$$P_{m,n}(\mu) = \left[(2n+1)\,\frac{(n-m)!}{(n+m)!}\right]^{\frac{1}{2}} \frac{(1-\mu^2)^{\frac{m}{2}}}{2^n\, n!}\,\frac{d^{n+m}}{d\mu^{n+m}}\,(\mu^2-1)^n, \qquad (4.2)$$

where $\mu=\sin\phi$. This definition applies to all integer values of m and n satisfying $n \geq |m|$ and it follows that

$$P_{-m,n}(\mu) = (-1)^m\, P_{m,n}(\mu) \qquad (4.3)$$

and that each of the functions may be written in the form

$$P_{m,n}(\mu) = (1-\mu^2)^{\frac{m}{2}}\, Q^{(1)}_{n-m}(\mu)\,, \qquad (4.4)$$

where $Q_{n-m}^{(1)}(\mu)$ is a polynomial in μ of degree n-m. Therefore the Legendre functions with order $m \geq 0$, which appear in (4.1), are symmetric with respect to the Equator when n-m is even and antisymmetric when n-m is odd. Furthermore it is seen that n-m is the number of zero points between the north pole and the south pole, and that the functions with $m \neq 0$ are zero at the poles. For $m=0$ the functions are simply the Legendre polynomials all of which are different from zero at the poles. The first few of the functions are given in Table 2.

Table 2

Normalized Legendre functions, $P_{m,n}(\mu)$

3	$\frac{\sqrt{7}}{2}(5\mu^3-3\mu)$	$\frac{\sqrt{21}}{4}(5\mu^2-1)\sqrt{1-\mu^2}$	$\frac{\sqrt{105}}{2\sqrt{2}}(\mu-\mu^3)$	$\frac{\sqrt{5}}{48}(1-\mu^2)^{3/2}$
2	$\frac{\sqrt{5}}{2}(3\mu^2-1)$	$\frac{\sqrt{15}}{\sqrt{2}}\mu\sqrt{1-\mu^2}$	$\frac{\sqrt{15}}{2\sqrt{2}}(1-\mu^2)$	
1	$\sqrt{3}\mu$	$\frac{\sqrt{3}}{2\sqrt{2}}\sqrt{1-\mu^2}$		
0	1			
n m	0	1	2	3

A number of recurrence relations are valid for the Legendre functions. We shall list only two of these both which will be used in the following, namely:

$$-\cos\phi\frac{dP_{m,n}}{d\phi} = -(1-\mu^2)\frac{dP_{m,n}}{d\mu}$$

$$= nD_{m,n+1}P_{m,n+1} - (n+1)D_{m,n}P_{m,n-1}\,, \qquad (4.5a)$$

$$\sin\phi\,P_{m,n} = \mu P_{m,n} = D_{m,n+1}P_{m,n+1} + D_{m,n}P_{m,n-1}\,, \qquad (4.5b)$$

where

$$D_{m,n} = \left(\frac{n^2 - m^2}{4n^2 - 1}\right)^{\frac{1}{2}} \quad . \tag{4.6}$$

Introducing the complex spherical harmonics:

$$Y_{m,n}(\lambda,\mu) = P_{m,n}(\mu)\, e^{im\lambda} \tag{4.7}$$

we may write the expansion (4.1) as

$$\begin{aligned} \psi(\lambda,\mu,t) &= \sum_{m=-\infty}^{\infty} \tilde{\psi}_m(\mu,t)\, e^{im\lambda} \\ &= \sum_{m=-\infty}^{\infty} \sum_{n=|m|}^{\infty} \tilde{\psi}_{m,n}(t)\, Y_{m,n}(\lambda,\mu) \quad , \end{aligned} \tag{4.8}$$

where the complex coefficients for $m \geq 0$ are given by

$$\begin{aligned} \tilde{\psi}_m(\mu,t) &= \tfrac{1}{2}\,(\tilde{\psi}_m^c(\mu,t) - i\,\tilde{\psi}_m^s(\mu,t)) \\ \tilde{\psi}_{m,n}(t) &= \tfrac{1}{2}\,(\tilde{\psi}_{m,n}^c(t) - i\,\tilde{\psi}_{m,n}^s(t)) \end{aligned} \tag{4.9}$$

(defining $\tilde{\psi}_0^s(\mu,t)=0$ and $\tilde{\psi}_{0,n}^s(t)=0$) and where the coefficients for negative and positive values of m are related by

$$\tilde{\psi}_{-m}(\mu,t) = \tilde{\psi}_m^*(\mu,t) \tag{4.10a}$$

$$\tilde{\psi}_{-m,n}(t) = (-1)^m\, \tilde{\psi}_{m,n}^*(t) \tag{4.10b}$$

with the asterisk denoting the complex conjugate. Eq. (4.10) follows from (4.3) and the fact that ψ is real.

We have seen in Section 2 that a particular equation in the space truncated system (e.g. the system (2.6)) is simplified considerably when the expansion functions are chosen to be orthogonal and when they are eigensolutions of the differential operator involved on the left-hand side of the corresponding partial differential equation. In our case these advantages can be obtained by choosing expansion functions which are eigensolutions of the Helmholtz equation:

$$\nabla^2 \Psi_n + \varepsilon_n \Psi_n = 0 \,, \tag{4.11}$$

where the spherical Laplacian is

$$\nabla^2( ) = \frac{1}{a^2\cos^2\phi}\left[\frac{\partial^2}{\partial\lambda^2}( ) + \cos\phi\frac{\partial}{\partial\phi}\left(\cos\phi\frac{\partial}{\partial\phi}( )\right)\right] . \tag{4.12}$$

Furthermore, it is an advantage to choose functions each of which satisfies the proper boundary conditions, which in our case follows from our assumptions about the smoothness of the true solution at any point on the sphere and particularly at the pole points. Because if this is the case then any expansion in terms of such functions will automatically satisfy the boundary conditions. The main reason for choosing the surface spherical harmonics is that these functions do have these advantageous properties. Except for a constant factor they are the only non-trivial solutions to (4.11) with continuous derivatives up to the second order over the entire sphere (*e.g. Courant and Hilbert*, 1953). The eigenvalues are uniquely determined to be $\epsilon_n = n(n+1)/a^2$ and the functions $Y_{m,n}(\lambda,\mu)$ form a complete system of orthogonal functions on the sphere. Thus, the spherical harmonics satisfy

$$\nabla^2 Y_{m,n} = -\frac{n(n+1)}{a^2} Y_{m,n} \tag{4.13}$$

and with the normalization factor chosen in (4.2) the orthogonality condition is

$$\frac{1}{4\pi}\int_0^{2\pi}\int_{-1}^{1} Y_{m,n}(\lambda,\mu)Y^*_{m',n'}(\lambda,\mu)\,d\mu d\lambda = \begin{cases} 1 \text{ for } (m,n)=(m',n'), \\ 0 \text{ for } (m,n)\neq(n',m'). \end{cases} \tag{4.14}$$

We note that in view of (3.11) the condition (4.14) implies that

$$\tfrac{1}{2}\int_{-1}^{1} P_{m,n}(\mu)\,P_{m',n'}(\mu)\,d\mu = \begin{cases} 1 \text{ for } n=n' \\ 0 \text{ for } n\neq n' \end{cases}, \tag{4.15}$$

Consistent with (3.11) and (4.14) the expansion coefficients in (4.8) are determined by

$$\tilde{\psi}_m(\mu,t) = \frac{1}{2\pi}\int_0^{2\pi} \psi(\lambda,\mu,t)\,e^{-im\lambda}\,d\lambda\,, \tag{4.16a}$$

$$\tilde{\psi}_{m,n}(t) = \frac{1}{4\pi}\int_0^{2\pi}\int_{-1}^{1} \psi(\lambda,\mu,t)\,Y^*_{m,n}(\lambda,\mu)\,d\mu d\lambda\,. \tag{4.16b}$$

Following *Platzman* (1960) we have chosen the normalization factor in (4.2) so that the mean square integral of each spherical harmonic over the sphere is unity as expressed by (4.14). Unfortunately a number of different normalization factors are used in the literature. Obviously the values of the expansion coefficients depend upon the choice of normalization and it should be noted that if the normalization factor in (4.2) is changed then the expressions (4.3), (4.6), (4.10a). (4.14), (4.15) and (4.16b) must be changed accordingly.

As mentioned above series expansions in terms of spherical harmonics converge very fast for sufficiently smooth functions. So, Parseval's equation

$$\sum_{n=0}^{\infty}\sum_{m=-n}^{n} |\tilde{\psi}_{m,n}|^2 = \frac{1}{4\pi}\int_{-1}^{1}\int_0^{2\pi} (\psi(\lambda,\mu))^2\,d\lambda d\mu \tag{4.20}$$

shows that the coefficients $\tilde{\psi}_{m,n}$ must tend towards zero for $n \to \infty$. For most reasonably smooth functions, the convergence is actually much faster than required by (4.20). In particular, if ψ is infinitely differentiable one may (*see Orszag*, 1974) show that the remainder in the series (4.17) after N terms converges uniformly towards zero faster than any finite power of 1/N.

4.3 Types of truncation

The spectral method for global models is based on truncated series of spherical harmonics. For the stream function for instance the infinite series (4.8) must be truncated. This truncation is not as straightforward as in the one-dimensional case considered in Section 3, because the series involves a summation over two indices. As the dependent variables are real functions the relation (4.b) applies. Therefore, if a complex component $\psi_{m,n}Y_{m,n}$ is included in the truncated series then the component $\psi_{-m,n}Y_{-m,n}$ must also be included. We need therefore only consider the truncation for $m \geq 0$. When truncating (4.8) we shall require that all retained real components, (4.19), must be able to move in the zonal direction which implies that the complex components must have a real as well as an imaginary part. The complex components with $m \geq 0$ in the infinite series may be represented by points in an m,n - diagram as that in Fig. 9. The infinite number of components is represented by the points in the half plane $n > 0$ with integer values of m and n situated at and above the line $n = m$.

In particular two different types of truncation have been used. Namely, the triangular truncation where all components with $n > N$ are set equal to zero and the parallelogrammic truncation where all components with $|m| > M$ or $n > |m| + J$ are set equal to zero. Here N, M and J are positive integer constants. When using the triangular truncation the truncated series takes the form

$$\hat{\psi}(\lambda,\mu,t) = \sum_{m=-N}^{N} \sum_{n=|m|}^{N} \psi_{m,n}(t)\, Y_{m,n}(\lambda,\mu) \qquad (4.22)$$

and when using the parallelogrammic truncation it takes the form

$$\hat{\psi}(\lambda,\mu,t) = \sum_{m=-M}^{M} \sum_{n=|m|}^{|m|+J} \psi_{m,n}(t)\, Y_{m,n}(\lambda,\mu)\,. \qquad (4.23)$$

Usually M is chosen equal to J in which case the latter truncation is termed a rhomboidal truncation. In Fig. 9 the truncation limits are indicated for a triangular and a rhomboidal truncation which have approximately the same number of degrees of freedom.

A triangular truncation has the property that the resolution is uniform over the sphere. This follows from the fact that if we introduce a new spherical coordinate system, obtained from the usual system, by an arbitrary rotation around an arbitrary axis through the centre of the sphere, then a spherical harmonic of degree n in the usual system can be expressed as a linear combination of spherical harmonics in the new system, all of which are of the degree n. This relation may be written

$$Y_{m,n}(\lambda,\phi) = \sum_{m'=-n}^{n} C_n^{(m,m')}\, Y_{m',n}(\lambda',\mu') ,$$

where λ' and ϕ' are the coordinates in the new system ($\mu'=\sin\phi'$) and where the complex coefficients $C_n^{(m,m')}$ depend on n, m, m' and on the relative orientation of the new coordinate system with respect to the usual system. (*See Courant and Hilbert*, 1953, for further details). It follows that an expansion truncated at degree N remains truncated at degree N in any spherical coordinate system. The resolution in an area on the surface of the sphere can therefore neither depend on direction nor can it depend on the position of the area.

The rhomboidal truncation is invariant to arbitrary rotations around the Earth's axis, so the representation must be uniform in the zonal direction. In the meridional direction, however, the resolution is found to vary.

The choice of the type of truncation may be based upon analysis of atmospheric data. This approach was used by *Ellsaesser* (1966) who introduced the rhomboidal truncation. He presents a single spherical harmonic analysis of northern hemisphere kinetic energy at 500 mb, which indicates that for the case considered and at least for relatively small values of M a maximum amount of variance

with a minimum number of components is obtained with a rhomboidal truncation. A more extensive analysis made by *Baer* (1972) of northern hemisphere kinetic energy, based upon data from two winter months and several levels, indicates, however, that for smaller scales the isopleths of constant energy in the mean tend to follow lines of constant n considerably more closely than lines of constant m and constant n-m. This result suggests that the appropriate truncation should be triangular rather than rhomboidal. The approximate form of the isopleths, as presented by *Baer* (1972), is indicated by the dot-dashed curve in Fig. 9.

4.4 The non-divergent barotropic vorticity equation

4.4.1 Introduction

In this sub-section we shall illustrate the application of the spectral method in spherical geometry by considering the vorticity equation in the simple case of non-divergent, barotropic motion. Basically we choose this equation because of its simplicity and because of its relevance for large scale atmospheric dynamics, but also because it is a convenient starting point for extensions to more complex models. From a historical point of view it was also the first meteorological equation to which the spectral method was applied.

For non-divergent barotropic motion the stream function may be considered the only dependent variable and the vorticity equation may be written

$$\frac{\partial \zeta}{\partial t} = - \nabla \cdot \eta \vec{V}_{\psi} \quad , \tag{4.24}$$

where $\zeta = \nabla^2 \psi$ is the relative vorticity, $\eta = \zeta + f$ is the absolute vorticity and the non-divergent velocity is given by $\vec{V}_{\psi} = \vec{k} \times \nabla \psi$. Here $f = 2\Omega\mu$ is the Coriolis parameter, $\vec{k}$ the vertical unit vector and Ω the Earth's angular velocity.

4.4.2 Properties of the true solution

The true solution to (4.24) satisfies the following three important integral constraints

$$\frac{d\overline{M}}{dt} = 0 \ , \tag{4.25a}$$

$$\frac{d\overline{K}}{dt} = 0 \ , \tag{4.25b}$$

$$\frac{d\overline{E}}{dt} = 0 \ , \tag{4.25c}$$

where the bar indicates a global mean value defined by

$$\overline{(\ )} = \frac{1}{4\pi} \int_0^{2\pi} \int_{-1}^{1} (\ )\, d\lambda d\mu \equiv \frac{1}{S} \int_S (\ )\, dS \tag{4.26}$$

and where $M = u\, a \cos\phi$ is the angular velocity around the Earth's axis, $K = \frac{1}{2}\vec{V}_\psi^{\,2}$ is the kinetic energy per unit mass and $E = \frac{1}{2}\zeta^2$ is the enstrophy per unit mass.

The constraints (4.25) are valid also for the approximate solution to (4.24) determined by the corresponding truncated system of spectral equations, which will be derived in the following subsection.

4.4.3 The truncated spectral equations

We write (4.24) in the form

$$\frac{\partial}{\partial t} \nabla^2\psi = - \frac{2\Omega}{a^2} \frac{\partial \psi}{\partial \lambda} + F(\psi) \ , \tag{4.30}$$

where

$$F(\psi) = \frac{1}{a^2} \left(\frac{\partial \psi}{\partial \mu} \frac{\partial}{\partial \lambda} \nabla^2\psi - \frac{\partial \psi}{\partial \lambda} \frac{\partial}{\partial \mu} \nabla^2\psi \right) . \tag{4.31}$$

We seek an approximate solution in terms of a truncated series of spherical harmonics and choose the triangular truncation (4.22), although any other type of truncation might have been used. The following derivations are dependent upon the choice of truncation but they are easily modified to apply to any other type of truncation.

Generally a truncated series of the form (4.22) will not satisfy (4.24) exactly. This follows from the fact that the equation includes a nonlinear term as well as linear terms. The situation is quite analogous to that for the nonlinear advection considered in Section 3. When substituting (4.22) into the equation each of the terms becomes a truncated series, but the nonlinear term includes more components than the linear terms. For the left-hand side term, by using (4.13), we get

$$\frac{\partial}{\partial t} \nabla^2 \hat{\psi} = - \sum_{m=-N}^{N} \sum_{n=|m|}^{N} \epsilon_n \frac{d\psi_{m,n}}{dt} Y_{m,n} \quad , \tag{4.32}$$

where $\epsilon_n = n(n+1)/a^2$ and for the linear term on the right-hand side we get

$$- \frac{2\Omega}{a^2} \frac{\partial \hat{\psi}}{\partial \lambda} = - \frac{2\Omega}{a^2} \sum_{m=-N}^{N} \sum_{n=|m|}^{N} im\psi_{m,n} Y_{m,n} \quad . \tag{4.33}$$

For the nonlinear term on the other hand we get

$$F(\hat{\psi}) = \sum_{m=-2(N-1)}^{2(N-1)} \sum_{n=|m|}^{2(N-1)} F_{m,n} Y_{m,n} \quad , \tag{4.34}$$

where

$$F_{m,n} = \frac{1}{4\pi} \int_0^{2\pi} \int_{-1}^{1} F(\hat{\psi}) \, Y^*_{m,n} \, d\lambda d\mu \quad . \tag{4.35}$$

Thus, when the truncated series $\hat{\psi}$ given by (4.22) is substituted into the partial differential equation (4.30) we will get a residue which generally does not vanish identically. In accordance with the general procedure outlined in Section 2, we determine a truncated system of spectral equations by minimizing the mean square residue. This is achieved by applying the operator (4.21) on both sides

of the equation. Using the orthonormality relation (4.14) and(4.32) - (4.34) this procedure immediately gives the system

$$\frac{d\psi_{m,n}}{dt} = \frac{2\Omega m}{n(n+1)} i\psi_{m,n} - \frac{a^2}{n(n+1)} F_{m,n} \qquad (4.43)$$

$$\text{for } 0 \leqq |m| \leqq n \leqq N \text{ (and } n \neq 0).$$

The true value of $\partial\zeta/\partial t$ in the special case $\psi=\hat{\psi}$ is

$$\left(\frac{\partial \zeta}{\partial t}\right)_{\psi=\hat{\psi}} = - \frac{2\Omega}{a^2} \frac{\partial \hat{\psi}}{\partial \lambda} + F(\hat{\psi})$$

which, using (4.33) and (4.34), may be written

$$\left(\frac{\partial \zeta}{\partial t}\right)_{\psi=\hat{\psi}} = - \frac{2\Omega}{a^2} \sum_{m=-N}^{N} \sum_{n=|m|}^{N} im\psi_{m,n} Y_{m,n}$$

$$+ \sum_{m=-2(N-1)}^{2(N-1)} \sum_{n=|m|}^{2(N-1)} F_{m,n} Y_{m,n} \,. \qquad (4.44)$$

The approximate value determined by the truncated system (4.43) is on the other hand

$$\frac{\partial \hat{\zeta}}{\partial t} = - \frac{2\Omega}{a^2} \sum_{m=-N}^{N} \sum_{n=|m|}^{N} im\, \psi_{m,n} Y_{m,n}$$

$$+ \sum_{M=-N}^{N} \sum_{n=|m|}^{N} F_{m,n} Y_{m,n} \,. \qquad (4.45)$$

Comparing (4.44) and (4.45) we see that the linear term, the so- called beta-term, is evaluated exactly from the truncated series representation of ψ whereas the components $F_{m,n}$ of the nonlinear term with $N < n \leq 2(N-1)$ are neglected in the approximate value determined by (4.45). Thus, aliasing is avoided and a cause of nonlinear instability is eliminated. Furthermore, as a consequence of this non-aliased truncation the integral constraints (4.25) which we found to be valid for the true solution are also valid for the solution to be truncated spectral equations. This was shown originally by *Lorenz* (1960) for plane geometry, using a representation in terms of double Fourier series, and by *Platzman* (1960) for spherical geometry. A less complicated proof based on the general property (2.9) of the spectral method may be found in *Machenhauer* (1979).

These conservation properties of the truncated spectral equation tends to conserve the gross characteristics of the energy spectrum and a systematic energy cascade towards higher wavenumbers is not possible. It should be noted that a certain blocking of energy in the highest wavenumbers, similar to that observed in Section 3.3.5 for the one-dimensional advection equation, is not excluded if at the same time energy is transferred to low wavenumbers. Furthermore, in actual numerical integrations the above constraints are of course only approximately valid due to time truncation and round-off errors. The effect of these errors can, however, usually be neglected.

Concerning the conservation of the mean angular momentum $\bar{M}$ we note that $\bar{M}$ is related to the coefficient $\psi_{0,1}$ by the relation

$$\bar{M} = -\frac{2}{\sqrt{3}} \psi_{0,1} ,$$

which follows from the definition (4.51a). Furthermore, the coefficient $\psi_{0,1}$, determines a solid rotating part of the velocity field defined by

$$u_{0,1} = -\frac{\partial}{a\partial\phi}(\psi_{0,1} P_{0,1}) = -\frac{\sqrt{3}}{a} \psi_{0,1} \cos\phi$$

or

$$u_{0,1} = \omega_{0,1} \, a \cos\phi ,$$

where

$$\omega_{0,1} = -\frac{\sqrt{3}}{a^2}\psi_{0,1} \ . \tag{4.52}$$

Thus, conservation of $\bar{M}$ implies that $\psi_{0,1}$ or in other words the solid rotating part of the velocity field is an invariant.

4.4.4 The interaction coefficient method

The linear term in (4.43) can easily be computed, but the problem is how to compute the non-linear term from (4.35). The original method was presented by *Silberman* (1954) and it was treated extensively in the papers by *Platzman* (1960) and *Baer and Platzman* (1961). This method, the so-called interaction coefficient method, builds upon a substitution of the expansion of ψ (4.22) into the expression for the nonlinear term (4.31) followed by a multiplication of the series. When the resulting series is substituted into (4.35) and the integration is carried out term by term we get

$$F_{m,n} = \frac{1}{a^2} \sum_{m_1=-N}^{N} \sum_{n_1=|m_1|}^{N} \sum_{m_2=-N}^{N} \sum_{\substack{n_2=|m_2| \\ n_2 > n_1}}^{N} i\psi_{m_1,n_1}\psi_{m_2,n_2} L_{n\, n_1 n_2}^{m\, m_1 m_2} \ , \tag{4.61}$$

where

$$L_{nn_1n_2}^{mm_1m_2} = \tfrac{1}{2}(\varepsilon_{n_2} - \varepsilon_{n_1}) \int_{-1}^{1} P_{m,n} \left(m_1 P_{m_1,n_1} \frac{dP_{m_2,n_2}}{d\mu} - m_2 P_{m_2,n_2} \frac{dP_{m_1,n_1}}{d\mu} \right) d\mu \tag{4.62}$$

$$\text{for } m = m_1 + m_2$$

$$\text{and } 0 \quad \text{for } m \neq m_1 + m_2$$

Even for moderately truncated representations the non-linear term is very laborious to compute from these expressions. As the numerical computation of the interaction coefficients defined in (4.62) is very time-consuming, these must be stored in the computer. Besides the interaction coefficients for $m \neq m_1 + m_2$ also a large number of those for $m = m_1 + m_2$ becomes zero and of course only the non-zero coefficients need to be stored, and to be included in the computation of (4.61). Even if only the nonzero interaction coefficients are considered the required storage and the required number of arithmetic operations involved in the computation of the non-linear term each time step increase very

fast with increasing resolution. *Orszag* (1970) estimates this increase to be approximately as N^5. As explained in the introduction to this chapter, this very fast increase was the reason why the spectral method for several years was considered not to be a realistic alternative to the grid point method for higher resolution integrations.

It was mentioned in the introduction that *Robert* (1966) developed an alternative method. In this method no interaction coefficients are used, so that the storage problem is reduced substantially. He uses the functions

$$G_p^m = (1-\mu^2)^{\frac{|m|}{2}} \mu^p e^{im\lambda} ,$$

where p is an integer larger than or equal to zero. We shall call these functions Robert functions. As any spherical harmonic may be written as a sum of these functions a truncated representation in terms of spherical harmonics may be transformed to a truncated representation in terms of Robert functions. The advantage of using these functions is that the product of two functions can be expressed in a simple form in comparison with the product of spherical harmonics. In Robert's method the calculation of each term in the equations is carried out separately and the results are added giving an array of coefficients for the time derivatives, which due to the non-linear terms contain coefficients outside the limit of the original truncations. This array is then truncated in such a way that the result is exactly equivalent to non-aliased truncations of the corresponding series of spherical harmonics. By this procedure no interaction coefficients are needed, and as mentioned above the storing space needed is reduced. A very rapid increase of required arithmetic operations with increasing resolution remains, however, a problem.

4.4.5 The transform method

As explained in the introduction to this chapter, the next step in the evolution of the spectral method was the introduction of the transform method, developed independently by *Orszag* (1970) and *Eliasen et al.* (1970). In this method the increase with increasing resolution of both storage and the number of arithmetic operations is reduced substantially. We shall illustrate the method by considering the computation of the non-linear term in (4.43). This term is determined by (4.35), which may split up into the following two integrals

$$F_{m,n} = \tfrac{1}{2} \int_{-1}^{1} F_m(\mu)\, P_{m,n}(\mu)\, d\mu \tag{4.63}$$

$$F_m(\mu) = \frac{1}{2\pi} \int_0^{2\pi} F(\hat{\psi}(\lambda,\mu))\, e^{-im\lambda}\, d\lambda \tag{4.64}$$

where

$$F(\hat{\psi}) = \frac{1}{a^2}\left(\frac{\partial\hat{\psi}}{\partial\mu}\,\frac{\partial\hat{\zeta}}{\partial\lambda} - \frac{\partial\hat{\psi}}{\partial\lambda}\,\frac{\partial\hat{\zeta}}{\partial\mu}\right) \tag{4.65}$$

and

$$\hat{\zeta} = \nabla^2\hat{\psi} \ . \tag{4.66}$$

Having chosen the triangular truncation $F_{m,n}$ is to be computed for $0 \le m \le n \le N$.

The idea was then to evaluate the above integrals with the aid of quadrature formulae, noting that this evaluation can be done exactly when proper quadrature formulae are chosen.

It was shown that the integrand in (4.64) for a certain μ is a truncated Fourier series in λ. The integral can therefore be computed exactly by the trapezoidal quadrature formulae (3.26) if a sufficient number of quadrature points are used. For the evaluation of the integral in (4.63) on the other hand, we choose the Gaussian quadrature formula.

$$\int_{-1}^{1} g(\mu)\, d\mu \sim \sum_{k=1}^{K} G_k^{(K)} \cdot g(\mu_k) \ , \tag{4.67}$$

where μ_k are roots of the Legendre polynomial $P_{0,K}(\mu)$ and the Gaussian coefficients are defined by

$$G_k^{(K)} = \frac{2(1-\mu_k^2)(2K-1)}{(KP_{0,K-1}(\mu_k))^2} \qquad (k=1,\ldots\ldots,K) \ .$$

This quadrature formulae is exact for any polynomial of degree smaller than or equal to 2K-1 (*cf. Krylov*, 1962). As was shown the integrand, $F_m(\mu)P_{m,n}(\mu)$, in (4.63) is in fact a polynomial in μ, so that computing the integral by means of Gaussian quadrature no approximation is introduced if a sufficient number of quadrature points is used. The reason for choosing the Gaussian and the trapezoidal formulae is that these quadratures are of the highest possible degree of precision for arbitrary polynomials and truncated Fourier series, respectively. (*Cf. Krylov*, 1962).

Using the Gaussian quadrature formula in (4.63) we obtain the expression $F_{m,n}$ for

$$F_{m,n} = \tfrac{1}{2} \sum_{k=1}^{K_2} G_k^{(K_2)} F_m(\mu_k) P_{m,n}(\mu_k), \tag{4.68}$$

where according to (4.64)

$$F_m(\mu_k) = \frac{1}{2\pi} \int_0^{2\pi} F(\hat{\psi}(\lambda,\mu_k)) e^{-im\lambda} \, d\lambda \ . \tag{4.69}$$

It is seen from the expression (4.34) that $F(\psi(\lambda,\mu_k))$ is a truncated Fourier series of maximum wavenumber equal to 2(N-1). The real and imaginary parts of the integrand, $F(\psi)e^{-im\lambda}$, in (4.69) are therefore both truncated Fourier series with maximum wavenumber 2(N-1)+m. Since we want to compute F_m for $0 \leq m \leq N$ it follows that for any m in question the integrand in (4.69) is a truncated Fourier series with maximum wavenumber at most equal to 3N-2. Using this result and the exactness property of the trapezoidal quadrature it follows that F_m can be evaluated exactly by

$$F_m(\mu_k) = \frac{1}{K_1} \sum_{j=1}^{K_1} F(\hat{\psi}(\lambda_j,\mu_k)) \, e^{-im\lambda_j} \qquad \text{for } 0 \leq m \leq N \tag{4.70}$$

and for any μ_k needed in (4.68) if K_1 is satisfying

$$K_1 \geq 3N-1 \ . \tag{4.71}$$

The integrand in (4.63), $F_m(\mu)P_{m,n}(\mu)$, for all $m \geq 0$ is found to be a polynomial of degree at most 2N-2+n. Since we need to compute $F_{m,n}$ only for $1 \leq n \leq N$ the integrand is for any n in question a polynomial of degree at most 3N-2. Now, the Gaussian quadrature (4.67) is exact for any polynomial of degree at most 2K-1. Consequently, the values of $F_{m,n}$ determined by (4.68) are exact if K_2 is chosen large enough to satisfy

$$K_2 \geq \frac{3N-1}{2} \ . \tag{4.72}$$

In order to use (4.70) at a certain Gaussian latitude circle $\mu=\mu_k$ the non-linear term $F(\hat{\psi})$ must be computed in the K_1 grid points (λ_j,μ_k); $j=1,2,\ldots,K_1$. These grid point values must be computed from the spherical harmonic coefficients $\psi_{m,n}(t)$, which are the history carrying quantities in the spectral model. So it remains to be shown how these can be computed.

Introducing the operators

$$\begin{aligned} \{\}^{(\lambda)} &= \frac{\partial}{\partial\lambda} \{\} \ , \\ \{\}^{(\mu)} &= -(1-\mu^2) \frac{\partial}{\partial\mu} \{\} \ , \end{aligned} \tag{4.73}$$

the non-linear term(4.65) may be written

$$F(\hat{\psi}) = \frac{1}{a^2(1-\mu^2)}\left(-\hat{\psi}^{(\mu)} \hat{\zeta}^{(\lambda)} + \hat{\psi}^{(\lambda)} \hat{\zeta}^{(\mu)}\right) \ . \tag{4.74}$$

The quantities in the parentheses may be computed by

$$\begin{aligned}
\hat{\psi}^{(\lambda)}(\lambda,\mu) &= \sum_{m=-N}^{N} \psi_m^{(\lambda)}(\mu)\, e^{im\lambda} \\
\hat{\psi}^{(\mu)}(\lambda,\mu) &= \sum_{m=-N}^{N} \psi_m^{(\mu)}(\mu)\, e^{im\lambda} \\
\hat{\zeta}^{(\lambda)}(\lambda,\mu) &= \sum_{m=-N}^{N} \zeta_m^{(\lambda)}(\mu)\, e^{im\lambda} \\
\hat{\zeta}^{(\mu)}(\lambda,\mu) &= \sum_{m=-N}^{N} \zeta_m^{(\mu)}(\mu)\, e^{im\lambda}
\end{aligned} \tag{4.75}$$

where

$$\begin{aligned}
\psi_m^{(\lambda)}(\mu) &= im \sum_{n=|m|}^{N} \psi_{m,n}\, P_{m,n}(\mu) \\
\psi_m^{(\mu)}(\mu) &= \sum_{n=|m|}^{N} \psi_{m,n}\, H_{m,n}(\mu) \\
\zeta_m^{(\lambda)}(\mu) &= im \sum_{n=|m|}^{N} \zeta_{m,n}\, P_{m,n}(\mu) \\
\zeta_m^{(\mu)}(\mu) &= \sum_{n=|m|}^{N} \zeta_{m,n}\, H_{m,n}(\mu)
\end{aligned} \tag{4.76}$$

Here

$$\zeta_{m,n} = -\frac{n(n+1)}{a^2}\, \psi_{m,n} \tag{4.77}$$

and

$$H_{m,n}(\mu) = -(1-\mu^2)\, \frac{dP_{m,n}}{d\mu} \quad . \tag{4.78}$$

The expressions (4.75) and (4.76) follow from application of the operators (4.73) to the expansions (4.22) and (4.47) of $\hat{\psi}$ and $\hat{\zeta}$. The functions $H_{m,n}(\mu)$, defined in (4.78), may be computed from the Legendre functions $P_{m,n}(\mu)$ using (4.5a).

We have now established all formulae necessary for the computation of the coefficients $F_{m,n}$ of the non-linear term from the coefficients $\psi_{m,n}$ by the transform method. The procedure may be summarised as follows:

Step 1 The vorticity components $\zeta_{m,n}$ are computed for $0 \leq m \leq n \leq N$ using (4.77).

In the following steps the contributions to (4.68) from the Gaussian latitudes μ_k; $k=1,2,\ldots,K_2$ are accumulated successively. The contribution from a certain Gaussian latitude $\mu=\mu_k$ is computed using the following steps:

Step 2 The Fourier coefficients $\psi_m^{(\lambda)}(\mu_k)$, $\psi_m^{(\mu)}(\mu_k)$, $\zeta_m^{(\lambda)}(\mu_k)$, and $\zeta_m^{(\mu)}(\mu_k)$ are computed for $0 \leq m \leq N$ using (4.76).

Step 3 The grid point values $\hat{\psi}^{(\mu)}(\lambda_j,\mu_k)\ldots$, $\hat{\zeta}^{(\mu)}(\lambda_j,\mu_k)$ are computed for $j=1,2,\ldots,K_1$ using (4.75).

Step 4 The non-linear term $\hat{F}(\lambda,\mu)$ is computed at the grid points (λ_j, μ_k); $j=1,2,\ldots,K_1$ using (4.74).

Step 5 The Fourier coefficients $F_m(\mu_k)$ of the non-linear term are computed for $0 \leq m \leq N$ using (4.70).

Step 6 The contribution to $F_{m,n}$ is computed for each coefficient with $0 \leq m \leq n \leq N$ by multiplying the Fourier component $F_m(\mu_k)$ with $\frac{1}{2}G_k^{(K_2)}P_{m,n}(\mu_k)$.

This successive accumulation procedure has the advantage that storage of grid point values at any time is only required for a single Gaussian latitude.

We see that the method involves a transformation from the spectral domain to the physical space grid points, and a computation of the non-linear term in the physical space followed by a transformation of the non-linear term to the spectral domain. The grid in the physical space, the so-called transform grid, is the intersection of the K_1 equally spaced longitudes $\lambda=\lambda_j$ and the K_2 Gaussian latitudes $\mu=\mu_k$ (which are almost equally spaced in ϕ).

The total number of arithmetic operations involved in the transform method may be counted for each step in the procedure described above. In such counts a multiplication and an addition of real numbers are usually counted each as half an operation (*Orszag*, 1970). Such counts show (*cf.*, *Machenhauer and Rasmussen*, 1972) that for large values of N the number of operations involved in step 1 and step 4 is proportional to N^2 and that those involved in the Legendre transformations in steps 2 and 6 are proportional to N^3. It is essential for the efficiency of the transform method that a Fast Fourier Transform (FFT) algorithm (*Cooley and Tukey*, 1965) can be used in the Fourier transforms involved in step 3 and step 5. The number of arithmetic operations involved in each FFT is proportional to $K_1 \log K_1$. This implies that if N is the maximum value satisfying (4.72) then when using FFT the number of operations involved in step 3 and step 5 becomes proportional to $N^2 \log N$ for large values of N. So far it has not been possible to find an algorithm which, in analogy with the FFT, cuts down the rate of increase of the number of operations involved in the Legendre transforms in step 2 and step 6. A certain reduction in the number of operations can be obtained in global models, at the expense of extra storage, by taking advantage of the fact that the Legendre functions are either symmetric or antisymmetric with respect to the equator. The rate of increase for large N is, however, unchanged so that the total number of operations involved in the computation of the non-linear term will be dominated by the number of operations involved in the Legendre transformations when N is large and therefore become approximately proportional to N^3. This is still a considerably reduced rate of increase compared to that of the interaction coefficient method. Instead of an increase proportional to N^5 we have an increase proportional to N^3 for large values of N. It should be noted, however, that in practice, even for the high resolution models used at present for medium range weather predictions, models are far from the asymptotic limit. This is due to the dominance of grid point calculations, as the parameterization of physical processes, which for such models are included in step 4 and for which the increase is proportional to N^2. For the sake of completeness it should be mentioned that for very small values of N the interaction coefficient method becomes the most efficient method, in terms of number of operations involved.

Whilst the Legendre transforms can be considered inefficient relative to the FFT the direct use of (4.68) and (4.76) greatly facilitates computer coding of the transform method, using the successive accumulation at each Gaussian latitude described above. Even if a fast Legendre transform could be found it seems unlikely that it would be used in more complex multi-level models, as it would necessitate simultaneous grid point representation of the full two dimensional grid or alternatively substantial peripheral device usage.

4.5 Extensions to primitive equations models

4.5.1 Introduction

It was shown by *Merilees* (1968) that the spectral method in principle may be applied to multi-level pressure coordinate models if the differentiated forms of the equation of motion are used. In this stream function ψ and velocity potential χ may be used as the prognostic variables describing the velocity fields. Neglecting forcing and friction terms Merileees shows that three types of non-linear terms appear in the equations, namely terms of the form $\vec{k}\times\nabla A\bullet\nabla B$, $\nabla A\bullet\nabla B$ and AB, where A and B are scalar variables. Corresponding to these different terms three types of interaction coefficients arise, one of which is the coefficients defined in (4.62). The storage problem with the interaction coefficient method for a more general model than the non-divergent barotropic model considered in subsection 4.4 becomes therefore even more obvious. The transform method may, however, be used also for such models as each of the three types of non-linear terms becomes truncated series of spherical harmonics (*cf. Eliasen et al.*, 1970). If the triangular type of truncation is used for all variables then the non-linear terms become truncated series with $0\leq|m|\leq n\leq 2N$. Consequently the number of Gaussian latitudes, K_2, and equally spaced longitudes, K_1, to be used in the transform grid must satisfy

$$K_1 \geq 3N+1 \quad \text{and} \quad K_2 \geq \frac{3N+1}{2} \tag{4.79}$$

respectively. When using parallelogrammic truncations, the numbers must satisfy

$$K_1 \geq 3M+1 \quad \text{and} \quad K_2 \geq \frac{2M+3J+1}{2} \; . \tag{4.80}$$

Concerning integral constraints of pressure-coordinate models it follows from *Merilees* (1968) that when the lower boundary is assumed to be isobaric surface at which $\omega=dp/dt=0$ and an energetically consistent vertical discretization is used then the spectral truncation does not disturb the energy

consistency. This property of the spectral method is due to the fact that the total energy for such models, just as for the non-divergent barotropic model, is a quadratic quantity in variables represented by spherical harmonics. The non-aliased truncation of the non-linear terms, therefore, implies quasi-conservation of energy in adiabatic friction-free integrations in the same way as for the non-divergent barotropic model.

Most non-balanced spectral models used at present are based on the general system of equations in sigma- or hybrid-coordinates (*Simmons and Burridge*, 1981). For such models the mean kinetic energy is a cubic quantity in variables, which are expanded in terms of spherical harmonics and consequently a non-aliased truncation of non-linear terms does not automatically imply quasi-conservation of the total energy. *Weigle* (1972) has made a detailed study of the conservation properties of a shallow water model (the simplest sigma-coordinate model). He demonstrated that the time derivative of the total energy, determined by the truncated set of spectral equations, in general is non-zero. In other words, quasi-conservation of total energy is not automatically ensured in a spectral shallow water model. In practice, however, experiments with this model as well as with more general sigma-level models have shown that the total energy is very nearly conserved during adiabatic friction-free integrations (*cf. Eliasen et al.*, 1970, *Bourke*, 1972; 1974, *Hoskins and Simmons*, 1975 and *Baede et al.*, 1976).

When using the differentiated forms of the equations of motion, that is, the vorticity and divergence equations, only true scalar variables are involved and no problems are encountered in representing the variables in terms of spherical harmonics. Concerning systems of equations with the equations of motion in the momentum form the question arises as to how the horizontal velocity field should be represented in the spectral domain. As discussed in Subsection 4.2 the velocity components, u and v, themselves should not be represented by truncated series of spherical harmonics, because both components generally are discontinuous at the poles.

Robert (1966) succeeded in making the first spectral integration of a model based on the equations of motion in the momentum form. He uses a representation of the velocity components, u and v, which is equivalent to a truncated representation of the stream function ψ and the velocity potential χ in terms of surface spherical harmonics. Such a representation automatically fulfils the proper boundary conditions at the poles. Using this representation of u and v, without any truncation in the meridional representation. These untruncated tendencies are then converted to the equivalent ten-

dencies in ψ and χ, which are finally truncated. The spectral computations are made using the Robert functions mentioned in Subsection 4.4.4 and the computations are rather time consuming as all the components in the non truncated meridional representation of the tendencies have to be computed. He had, however, shown that the spectral method could be used also for the momentum form of the equations of motion.

Eliasen et al. (1970) used the same principles as Robert in the integration of a spectral barotropic, primitive equation model, i.e. a shallow water model. But here the variables were represented directly in spherical harmonics. In the following Subsection the method introduced by these authors will be presented.

4.5.2 An u-/v-equation model

given the representation of a velocity field by the truncated series of the stream function ψ and the velocity potential χ:

$$\chi: \quad \hat{\psi} = \sum_{m=-N}^{N} \sum_{n=|m|}^{N} \psi_{m,n} Y_{m,n}, \qquad \hat{\chi} = \sum_{m=-N}^{N} \sum_{n=|m|}^{N} \chi_{m,n} Y_{m,n}, \tag{4.81}$$

the equivalent representations of u and v, determined from the definitions

$$u = \frac{1}{a \cos\phi}\left(\frac{\partial\chi}{\partial\lambda} - \cos\phi \frac{\partial\psi}{\partial\phi}\right), \qquad v = \frac{1}{a \cos\phi}\left(\frac{\partial\psi}{\partial\lambda} + \cos\phi \frac{\partial\chi}{\partial\phi}\right) \tag{4.82}$$

are

$$\hat{u} = \frac{\hat{U}}{\cos\phi}; \quad \hat{U} = \sum_{m=-N}^{N} \sum_{n=|m|}^{N+1} U_{m,n} Y_{m,n}, \qquad \hat{v} = \frac{\hat{V}}{\cos\phi}; \quad \hat{V} = \sum_{m=-N}^{N} \sum_{n=|m|}^{N+1} V_{m,n} Y_{m,n}, \tag{4.83}$$

where the coefficients $U_{m,n}$ and $V_{m,n}$ are determined from the coefficients $\psi_{m,n}$ and $\chi_{m,n}$ by the relations

$$U_{m,n} = \frac{1}{a}\{(n-1)\, D_{m,n}\, \psi_{m,n-1} + im\chi_{m,n} - (n+2) D_{m,n+1}\psi_{m,n+1}\}\,, \tag{4.84}$$

$$V_{m,n} = \frac{1}{a}\{(1-n)\, D_{m,n}\, \chi_{m,n-1} + im\psi_{m,n} + (n+2)\, D_{m,n+1}\, \chi_{m,n+1}\}\,.$$

The relations (4.83) and (4.84) are easily derived by substituting (4.81) into (4.82) and by making use of the relation (4.5). It is seen from (4.83) that u and v are represented by truncated series of spherical harmonics, $\hat{U}$ and $\hat{V}$, divided by $\cos\phi$. We note that the series $\hat{U}$ and $\hat{V}$ extend to one more degree above that for $\hat{\psi}$ and $\hat{\chi}$. When the series $\hat{\psi}$ and $\hat{\chi}$ are given then the series $\hat{U}$ and $\hat{V}$ can easily be computed from the above relations (4.84) and the velocity field determined by (4.83) will then automatically be a smooth continuous field all over the globe, including the pole points. It is obvious that this must imply certain relations between the coefficients $U_{m,n}$ and $V_{m,n}$ as the number of these coefficients is larger than the number of coefficients $\psi_{m,n}$ and $\chi_{m,n}$ from which they are determined. Such relations were derived by *Eliasen et al.* (1970), who called them truncation relations. *Orszag* (1974) and *Byrnak* (1975) have later shown that these relations are equivalent to boundary conditions at the poles and that such relations must be satisfied even for infinite series, if the velocity field to be described is a smooth (infinitely differentiable) vector field.

It follows from the derivation that these relations must be valid also in the special case when ψ and χ can be represented by truncated series as those given in (4.81) in which case the following relations are obtained between the coefficients in (4.83):

$$\sum_{n=|m|}^{\infty} (\delta_A^{(n-m)} \tilde{U}_{m,n} + \delta_S^{(n-m)}\, i\, \tilde{V}_{m,n})\, C_{m,n} = 0\,, \tag{4.90a}$$

$$\sum_{n=|m|}^{\infty} (\delta_S^{(n-m)} \tilde{U}_{m,n} + \delta_A^{(n-m)}\, i\, \tilde{V}_{m,n})\, C_{m,n} = 0\,, \tag{4.90b}$$

where

$$\delta_A^{(n-m)} = \begin{cases} 1 & \text{for } n-m \text{ odd} \\ 0 & \text{for } n-m \text{ even} \end{cases}$$

and

$$\delta_S^{(n-m)} = \begin{cases} 0 & \text{for } n-m \text{ odd} \\ 1 & \text{for } n-m \text{ even} \end{cases} .$$

Condition (4.90a) relates the coefficients describing the symmetric part of the velocity field (that is, U symmetric and V antisymmetric with respect to the Equator) and (4.90b) relates the coefficients describing the antisymmetric velocity field.

As U and V are both real fields it suffices to consider the relations for $m \geq 0$. In the case $m = o$ the coefficients $U_{0,n}$ and $V_{0,n}$ are real numbers and as the real and imaginary parts on the left-hand side of (4.91) must vanish separately we get the following four relations

$$\begin{aligned}
&\sum_{n=0}^{N+1} \delta_A^{(n-m)} C_{0,n}\, U_{0,n} = 0 , \\
&\sum_{n=0}^{N+1} \delta_S^{(n-m)} C_{0,n}\, V_{0,n} = 0 , \\
&\sum_{n=0}^{N+1} \delta_S^{(n-m)} C_{0,n}\, U_{0,n} = 0 , \\
&\sum_{n=0}^{N+1} \delta_A^{(n-m)} C_{0,n}\, V_{0,n} = 0 .
\end{aligned} \qquad (4.92)$$

Choosing the arbitrary constants

$$C_{m,N+1} = -1 ,$$

then the values of $C_{m,n}$ for $n \leq N$ are given by

$$C_{m,n} = \left(\frac{2n+1}{2N+3} \frac{(N-m+1)\ (N-m)\ (N-m-1)\ldots.(n-m+1)}{(N+m+1)\ (N+m)\ (N+m-1)\ldots.(n+m+1)} \right)^{\frac{1}{2}}$$

(see *Byrnak*, 1975).

By using the representations (4.83) for u and v, truncated spectral forms of the primitive equations of motion may be derived. We shall illustrate the procedure by considering the shallow water model equations. Substituting

$$u = \frac{U}{\cos\phi} \quad \text{and} \quad v = \frac{V}{\cos\phi}$$

these may be written

$$a\frac{\partial U}{\partial t} = \underbrace{\frac{1}{1-\mu^2}\left[-UU^{(\lambda)} + VU^{(\mu)}\right]}_{F_1(\lambda,\mu)} + 2\Omega a\mu V - \phi^{(\lambda)} ,$$

$$a\frac{\partial V}{\partial t} = \underbrace{\frac{1}{1-\mu^2}\left[-UV^{(\lambda)} + VV^{(\mu)} - (U^2+V^2)\mu\right]}_{F_2(\lambda,\mu)} - 2\Omega a\mu U + \phi^{(\mu)} , \quad (4.93)$$

$$a\frac{\partial \Phi}{\partial t} = \underbrace{\frac{1}{1-\mu^2}\left[-U\Phi^{(\lambda)} + V\Phi^{(\mu)} - \Phi U^{(\lambda)} + \Phi V^{(\mu)}\right]}_{F_3(\lambda,\mu)} ,$$

where the operators introduced in (4.73) are used. Substituting the series $\hat{U}$, $\hat{V}$ given by (4.83) and the series

$$\hat{\Phi} = \sum_{m=-N}^{N} \sum_{n=|m|}^{N} \Phi_{m,n} Y_{m,n}$$

for U,V and Φ respectively and applying the operator $\{\}_{m,n}$, defined in (4.21), to each of the equations we obtain the following set of spectral equations:

$$
\begin{aligned}
a\frac{dU_{m,n}}{dt} &= \{\hat{F}_1(\lambda,\mu)\}_{m,n} + 2\Omega a(D_{m,n}V_{m,n-1} + D_{m,n+1}V_{m,n+1}) - im\Phi_{m,n} \,, \\
a\frac{dV_{m,n}}{dt} &= \{\hat{F}_2(\lambda,\mu)\}_{m,n} - 2\Omega a(D_{m,n}U_{m,n-1} + D_{m,n+1}U_{m,n+1}) \\
&\quad + ((n-1)D_{m,n}\Phi_{m,n-1} - (n+2)D_{m,n+1}\Phi_{m,n+1}) \,, \\
a\frac{d\Phi_{m,n}}{dt} &= \{\hat{F}_3(\lambda,\mu)\}_{m,n} \,,
\end{aligned}
\tag{4.94}
$$

where we have applied the relations (4.5) and the orthogonality condition (4.14).

The non-linear terms may be computed by the transform method described above for the advection term in the vorticity equation. For $\{F_1\}_{m,n}$ for example we have

$$
\begin{aligned}
\{F_1\}_{m,n} &= \tfrac{1}{2}\int_{-1}^{1} F1_m(\mu)\, P_{m,n}(\mu)\, d\mu \\
&= \tfrac{1}{2}\sum_{k=1}^{K_2} G_k^{(K_2)} F1_m(\mu_k)\, P_{m,n}(\mu_k) \,,
\end{aligned}
$$

where

$$
\begin{aligned}
F1_m(\mu_k) &= \frac{1}{2\pi}\int_0^{2\pi} \hat{F}_1(\lambda,\mu_k)\, e^{-im\lambda} d\lambda \\
&= \frac{1}{K_1}\sum_{j=1}^{K_1} \hat{F}_1(\lambda_j,\mu_k)\, e^{-im\lambda_j}
\end{aligned}
$$

and

$$
\hat{F}_1(\lambda_j,\mu_k) = \frac{1}{1-\mu_k^2}\left[-\hat{U}(\lambda_j,\mu_k)\hat{U}^{(\lambda)}(\lambda_j,\mu_k) + \hat{V}(\lambda_j,\mu_k)\,\hat{U}^{(\mu)}(\lambda_j,\mu_k)\right].
$$

The above procedure is analogous to that described in Subsection 4.4.5.

The truncation procedure must, however, be somewhat modified. If all the tendencies $(d/dt)U_{m,n}$ and $(d/dt)V_{m,n}$ within the given truncation limits were computed using (4.94), without any corrections, then the tendency field would not in general satisfy the pole conditions (4.91) and the field would not be a smooth vector function. Furthermore, if such a procedure were used in a pressure coordinate model the quasi-energy conservation property would be lost. On the other hand, if the truncation of the tendencies of U and V i carried out in such a way that it is equivalent to a non-aliased truncation of tendencies for the ψ and χ -fields, then a smooth vector function as well as quasi-energy conservation in pressure coordinate models are automatically obtained. Following *Robert* (1966) this principle was used by *Eliasen et al.* (1970). We shall briefly describe the truncation procedure developed by these authors.

Differentiating (4.84) with respect to time gives the relations

$$a\frac{dU_{m,n}}{dt} = (n-1)\,D_{m,n}\frac{d\psi_{m,n-1}}{dt} + im\frac{d\chi_{m,n}}{dt} - (n+2)\,D_{m,n+1}\frac{d\psi_{m,n+1}}{dt},$$

$$a\frac{dV_{m,n}}{dt} = (1-n)\,D_{m,n}\frac{d\chi_{m,n-1}}{dt} + im\frac{d\psi_{m,n}}{dt} + (n+2)\,D_{m,n+1}\frac{d\chi_{m,n+1}}{dt}. \qquad (4.95)$$

For each m we wish to truncate the time derivatives on the left-hand side in such a way that all contributions from the time derivatives $(d/dt)\psi_{m,n}$ and $(d/dt)\chi_{m,n}$ with $n > N$ are neglected. It is seen that this implies that all the time derivatives of $U_{m,n}$ and $V_{m,n}$ with $n > N+1$ shall be neglected. Concerning the time derivatives $(d/dt)U_{m,n}$ and $(d/dt)V_{m,n}$ with $n \leq N-1$ it is seen that they include only contributions from time derivatives of $\psi_{m,n}$ and $\chi_{m,n}$ which we want to retain. These time derivatives may, therefore, be computed directly, and without any correction from the spectral primitive equations (4.94). The four time derivatives of $U_{m,n}$ and $v_{m,n}$ for $n = N$ and $n = N+1$ on the other hand include contributions from the time derivatives of $\psi_{m,n}$ and $\chi_{m,n}$ with $n = N+1$ and $n = N+2$ which we want to neglect. The values of these time derivatives, computed from the primitive equations must therefore be corrected. It is obvious that such corrected tendencies must satisfy polar conditions similar to (4.91). For $m = 0$ this gives four relations corresponding to (4.92) from which the four corrected tendencies are determined by the time derivatives $(d/dt)U_{m,n}$ and

$(d/dt)V_{m,n}$ for $n < N$. For $m \neq 0$, however, we have only two relations, and we, therefore, have to correct two of the time derivatives in another way. From (4.95) it is seen that the corrected values $(d/dt)U^{cor}_{m,N}$ and $(d/dt)V^{cor}_{m,N}$ are given by

$$\frac{d}{dt} U^{cor}_{m,N} = \frac{d}{dt} U_{m,N} + \frac{1}{a} (N+2) D_{m,N+1} \frac{d}{dt} \psi_{m,N+1} ,$$

$$\frac{d}{dt} V^{cor}_{m,N} = \frac{d}{dt} V_{m,N} - \frac{1}{a} (N+2) D_{m,N+1} \frac{d}{dt} \chi_{m,N+1} , \qquad (4.96)$$

where the uncorrected values $d(U_{m,N})/dt$ and $d(V_{m,N})/dt$ can be determined from the primitive equations. Thus, if the time derivatives $d(\psi_{m,N+1})/dt$ and $d(\chi_{m,N+1})/dt$ can be determined in some other way then the corrected coefficients in (4.96) can be computed and the remaining two corrected coefficients can be computed from the relations corresponding to (4.91).

The method used by *Eliasen et al.* (1970) to compute $d(\psi_{m,N+1})/dt$ and $d(\chi_{m,N+1})/dt$, is based on the following relation

$$\{\alpha(A,B)\}_{m,n} = \tfrac{1}{2} \int_{-1}^{1} [imA_m(\mu) P_{m,n}(\mu) + B_m(\mu) H_{m,n}(\mu)] \frac{d\mu}{1-\mu^2} , \qquad (4.97)$$

Here A and B are some fields which are known to be zero at the poles. A_m and B_m are the Fourier coefficients

$$A_m(\mu) = \frac{1}{2\pi} \int_0^{2\pi} A(\lambda,\mu) e^{-im\lambda} d\lambda ,$$

$$B_m(\mu) = \frac{1}{2\pi} \int_0^{2\pi} B(\lambda,\mu) e^{-im\lambda} d\lambda , \qquad (4.98)$$

and the operator α is defined by

$$\alpha(A,B) = \frac{1}{1-\mu^2}\left(\frac{\partial A}{\partial \lambda} + (1-\mu^2)\frac{\partial B}{\partial \mu}\right). \tag{4.99}$$

In the derivation of (4.97) we have used integration by parts and the fact that B_m and A_m are zero at the poles. Noting that the vorticity $\zeta = \nabla^2\psi$ and the divergence $\delta = \nabla^2\chi$ may be written as

$$\begin{aligned} \nabla^2\psi &= \frac{1}{a}\alpha(V,-U)\,, \\ \nabla^2\chi &= \frac{1}{a}\alpha(U,V)\,, \end{aligned} \tag{4.100}$$

we obtain, by differentiating these expressions with respect to time and by using (4.97), the following relations

$$\frac{d\psi_{m,n}}{dt} = -\frac{a}{n(n+1)}\,\tfrac{1}{2}\int_{-1}^{1}\left\{im\frac{dV_m}{dt}P_{m,n} - \frac{dU_m}{dt}H_{m,n}\right\}\frac{du}{1-\mu^2}\,, \tag{4.101}$$

$$\frac{d\chi_{m,n}}{dt} = -\frac{a}{n(n+1)}\,\tfrac{1}{2}\int_{-1}^{1}\left\{im\frac{dU_m}{dt}P_{m,n} + \frac{dV_m}{dt}H_{m,n}\right\}\frac{du}{1-\mu^2}\,.$$

As the integrands are polynomials in μ the integrals can be computed using Gaussian quadrature, which gives the exact values if a sufficient number of latitudes is used. The values of the Fourier coefficients $d(U_m)/dt$ and $d(V_m)/dt$ to be used in the computations are easily obtained when the same Gaussian latitudes are used in the evaluation of the non-linear terms of the primitive equations (4.94). For the model considered it is found that in order to compute $d(\psi_{m,N+1})/dt$ and $d(\chi_{m,N+1})/dt$, which we need in (4.96), the number of longitudes K_1 and latitudes K_2 to be used in the transform grid must satisfy $K_1 \geq 3N+1$ and $K_2 \geq (3/2)N+1$ when triangular truncations are used and $K_1 \geq 3M+1$ and $K_2 \geq M+(3/2)J+1$ when parallelogrammic truncations are used.

4.5.3 A vorticity and divergence equations model

When using the grid point method it is a big advantage to use the u-/v- equations instead of the vorticity and divergence equations. The main reason for this fact is that it is a time consuming process to solve a Helmholtz equation when using the grid point method. With the spectral method based on spherical harmonics the basis functions have been chosen as eigensolutions of the Helmholtz equation and the solution therefore becomes a simple operation. *Bourke* (1972) has shown that a very efficient spectral model can be formulated using special forms of the vorticity and divergence equations. For the shallow water model he uses the prognostic equations

$$\frac{\partial \eta}{\partial t} = - \nabla \cdot \eta \vec{V} ,$$

$$\frac{\partial \delta}{\partial t} = \vec{k} \cdot \nabla \times \eta \vec{V} - \nabla^2 \left(\frac{\vec{V}^2}{2} + \Phi' \right) , \qquad (4.102)$$

$$\frac{\partial \Phi'}{\partial t} = -\nabla \cdot \Phi' \vec{V} - \bar{\Phi} \delta ,$$

where $\eta = \zeta + f = \nabla^2 \psi + 2\Omega \sin\phi$ is the absolute vorticity, $\delta = \nabla^2 \chi$ is the divergence and $\Phi = \bar{\Phi} + \Phi'$ is the geopotential at the free surface; $\bar{\Phi}$ denotes a time-independent global mean and Φ' denotes the deviation from the mean. The advantage of using the equations in this form is that the terms on the right-hand sides involve only the Laplacian operator or the α operator defined in (4.99), both of which are simple to handle when using spectral algebra. We shall consider a slightly changed version of Bourke's model following *Hoskins and Simmons* (1975) in the use of absolute vorticity and divergence instead of stream function and velocity potential as dependent variables.

The equations (4.102) may be written

$$\frac{\partial \eta}{\partial t} = - \frac{1}{a} \alpha(\eta U, \eta V) ,$$

$$\frac{\partial \delta}{\partial t} = \frac{1}{a} \alpha(\eta V, - \eta U) - \nabla^2 \left(\frac{U^2 + V^2}{2(1-\mu^2)} + \Phi' \right) , \qquad (4.103)$$

$$\frac{\partial \Phi'}{\partial t} = - \frac{1}{a} \alpha(\Phi' U, \Phi' V) - \bar{\Phi} \delta .$$

Using the triangular truncation, the following expansions are introduced

$$\hat{\eta} = \sum_{m=-N}^{N} \sum_{n=|m|}^{N} \eta_{m,n} Y_{m,n} , \tag{4.104a}$$

$$\hat{\delta} = \sum_{m=-N}^{N} \sum_{n=|m|}^{N} \delta_{m,n} Y_{m,n} , \tag{4.104b}$$

$$\hat{\Phi}' = \sum_{m=-N}^{N} \sum_{n=|m|}^{N} \Phi_{m,n} Y_{m,n} . \tag{4.104c}$$

The expansions for U and V corresponding to (4.104a) and (4.104b) are of the form (4.83) where relations between the coefficients $\eta_{m,n}$ and $\delta_{m,n}$ and the coefficients $U_{m,n}$ and $V_{m,n}$ are obtained from the relations (4.84).

These relations may be written

$$U_{m,n} = a \left(- \frac{1}{n} D_{m,n} \zeta_{m,n-1} - \frac{im}{n(n+1)} \delta_{m,n} + \frac{1}{n+1} D_{m,n+1} \xi_{m,n+1} \right) ,$$

$$V_{m,n} = a \left(\frac{1}{n} D_{m,n} \delta_{m,n-1} - \frac{im}{n(n+1)} \zeta_{m,n} - \frac{1}{n+1} D_{m,n+1} \delta_{m,n+1} \right) , \tag{4.105}$$

where we have used (4.13) together with the fact that $\hat{\zeta} = \nabla^2 \hat{\psi}$ and $\delta = \nabla^2 \chi$, which implies the relations

$$\zeta_{m,n} = - \frac{n(n+1)}{a^2} \psi_{m,n}$$

and

$$\delta_{m,n} = -\frac{n(n+1)}{a^2}\chi_{m,n}.$$

The coefficients $\zeta_{m,n}$ for the relative vorticity are identical to those for the absolute vorticity, $\eta_{m,n}$, except for (m,n) = (0,1). This follows from the relation $\eta = \zeta + 2\Omega\mu = \zeta + (2\Omega/\sqrt{3})P_{0,1}$, which implies that

$$\zeta_{m,n} = \begin{cases} \eta_{m,n} & \text{for } (m,n) \neq (0,1). \\ \eta_{m,n} - \frac{2\Omega}{\sqrt{3}} & \text{for } (m,n) = (0,1). \end{cases} \qquad (4.106)$$

The truncated spectral equations are obtained as usual by inserting the truncated expansions $\hat{\eta}, \hat{\delta}, \hat{\Phi}$ for the basic variables and those for the auxiliary variables $\hat{U}, \hat{V}$ and then applying the operator $\{\}_{m,n}$ on both sides of each equation, utilising the orthonormality of the spherical harmonics. The result is

$$\begin{aligned} \frac{d}{dt}\eta_{m,n} &= A_{m,n}\ , \\ \frac{d}{dt}\delta_{m,n} &= B_{m,n} + \varepsilon_n \Phi_{m,n}\ , \\ \frac{d}{dt}\Phi_{m,n} &= C_{m,n} - \bar{\Phi}\,\delta_{m,n}\ , \end{aligned} \qquad (4.107)$$

where the non-linear terms are determined by

$$\begin{aligned} A_{m,n} &= -\{\tfrac{1}{a}\alpha(\hat{\eta}\hat{U}, \hat{\eta}\hat{V})\}_{m,n}\ , \\ B_{m,n} &= \{\tfrac{1}{a}\alpha(\hat{\eta}\hat{V}, -\hat{\eta}\hat{U})\}_{m,n} + \varepsilon_n\{\frac{\hat{U}^2 + \hat{V}^2}{2(1-\mu^2)}\}_{m,n}\ , \\ C_{m,n} &= -\{\tfrac{1}{a}\alpha(\hat{\Phi}'\hat{U}, \hat{\Phi}'\hat{V})\}_{m,n}\ . \end{aligned} \qquad (4.108)$$

These terms are readily computed by the transform method using (4.104a), (4.104c), (4.105), (4.83), (4.98) and (4.97) where as usual the quadrature formulae (3.26) and (4.67) are used in the evaluation of the integrals involved. In order to avoid aliasing K_1 and K_2 must satisfy (4.79) or (4.80) if the truncation chosen is triangular or parallelogrammic.

For comparative purposes *Bourke* (1972) made a number of integrations with different rhomboidal truncations (M=J) using the transform method as well as the interaction coefficient method. The computation time per time step was measured for both methods and the results are presented in Figure 10, which clearly illustrates the computational advantage of the transform method.

A comparison of Bourke's transform model with the U and V model described in the preceding Subsection shows that for low to medium resolutions approximately the same number of arithmetic operations is involved. As, however, Bourke's model involves two more Legendre transforms than the U and V model should become less efficient for high resolutions. The two methods are of course equivalent methods of integrations as the U and V model simulates the truncation that would pertain to prognostics for vorticity and divergence. The truncation procedure is, however, more straightforward in Bourke's model, since the prognostic variables are true scalars. Another advantage with Bourke's model is that the implementation of a semi-implicit time scheme is facilitated by the explicit prognostic for divergence. Although more complicated, the semi-implicit time scheme may, however, also be incorporated in a U and V model (*Byrnak*, 1975).

For comparative purposes we shall consider the implementation of the semi-implicit time scheme to Bourke's model. We introduce a representation at discrete times and use the standard notation

$$\delta_t X = (X^{t+\Delta t} - X^{t-\Delta t})/2\Delta t \ , \qquad (4.109)$$

$$\overline{X}^t = \tfrac{1}{2} (X^{t+\Delta t} + X^{t-\Delta t}) \ .$$

In the semi-implicit scheme we use an averaging in time for the gravity wave terms and a centered time differencing for the time derivatives. This scheme gives

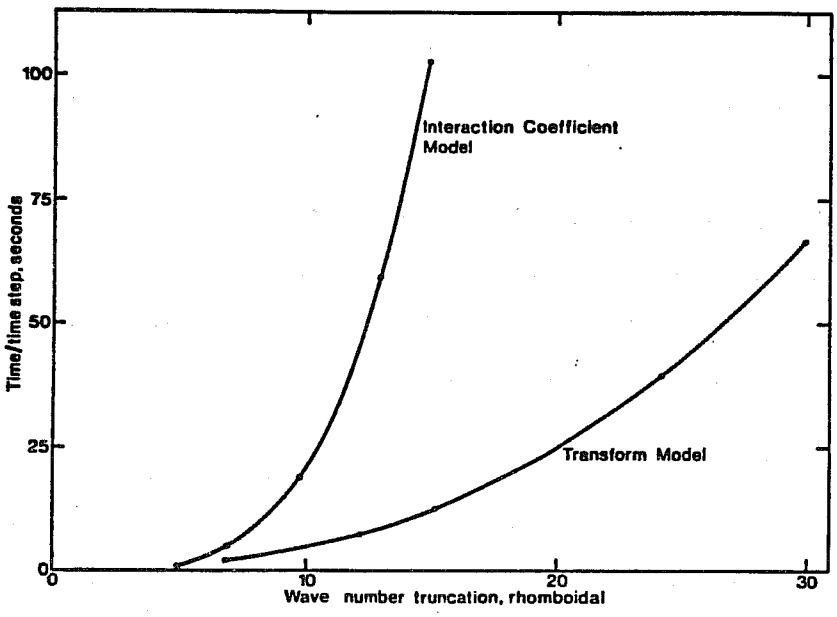

FIG.10 Computation time per time step (s) as a function of spectral resolution. Integrations of a global spectral model employing a transform method and employing the interaction coefficient method are compared (after Bourke (1972)).

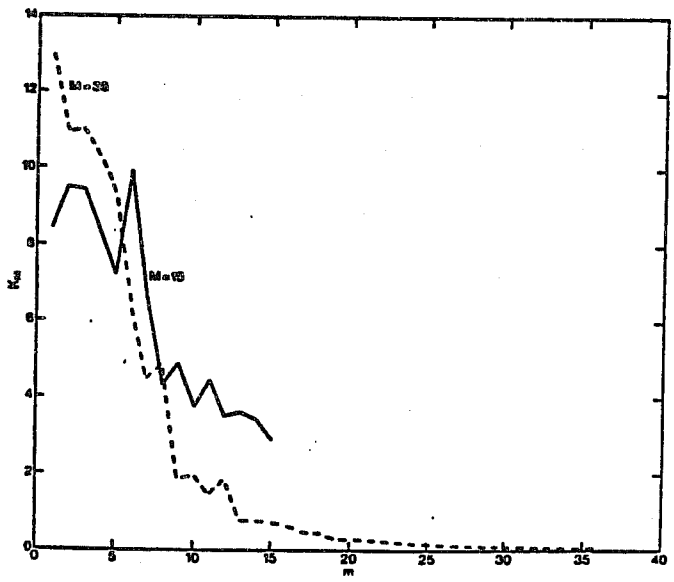

FIG. 11

Time averaged energy spectra from 8-day integrations of the non-divergent barotropic vorticity equation for two different rhomboidal truncations, M=15 and M=36.
Units: $m^2 s^{-2}$ (after Puri and Bourke (1974)).

$$\delta_t \eta_{m,n} = A^t_{m,n} ,$$

$$\delta_t \delta_{m,n} = B^t_{m,n} + \varepsilon_n \overline{\overline{\Phi}^t_{m,n}} , \qquad (4.110)$$

$$\delta_t \Phi_{m,n} = C^t_{m,n} - \overline{\Phi}\, \overline{\overline{\delta^t_{m,n}}} .$$

As the vorticity equation does not involve any gravity wave terms, the values $\eta^{t+\Delta t}_{m,n}$ are explicitly determined from the first equation. Using the relation $\delta_t X = (\overline{X}^t - X^{t-\Delta t})/\Delta t$ and eliminating from the last two equations, we get

$$\overline{\Phi}^t_{m,n} = \frac{1}{1+\varepsilon_n \Delta t^2 \overline{\Phi}} \{ \Phi^{t-\Delta t}_{m,n} + \Delta t \, (C^t_{m,n} - \overline{\Phi}\, \delta^{t-\Delta t}_{m,n}) - \Delta t^2 \overline{\Phi}\, B^t_{m,n} \} . \qquad (4.111)$$

Thus, for all spectral components $\overline{\overline{\Phi}^t_{m,n}}$ is determined explicitly by quantities known at the time considered. Once these values have been computed the values $\Phi^{t+\Delta t}_{m,n}$ and $\delta^{t+\Delta t}_{m,n}$ can be obtained directly from (4.109) and (4.110). Thus, for this model the semi-implicit scheme involves only very little extra computations each time step compared to an explicit scheme. On the other hand, for a grid point model the extra computations are much more extensive. For a grid point model we get instead of (4.111) an elliptic finite difference equation which is of the Helmholtz type. This equation must be solved every time step. The simplicity of (4.111) compared to the corresponding finite difference equation is obviously due to the fact that the spherical harmonics are eigensolution to the Helmholtz equation.

4.5.4 New variants of the spectral method

Recently a new variant of the transform method for the global shallow-water equations have been proposed. In the course of developing a semi-Lagrangian spectral model, *Ritchie* (1988) discarded the vorticity and divergence equations (since the latter does not lend itself to semi-Lagrangian

treatment), and returned to the prognostic equations (4.93) for U and V on the model's transform grid. Nevertheless he kept the spectral representation of vorticity, divergence and geopotential (4.104).

The values of the spectral coefficients $U_{m,n}$ and $V_{m,n}$ can be computed using (4.105). Using these coefficients and those of ϕ the gridpoint values of $\hat{U}$, $\hat{V}$, $\hat{U}^{(\lambda)}$, $\hat{V}^{(\lambda)}$, $\hat{\phi}$, $\hat{\phi}^{(\lambda)}$ and $\hat{\phi}^{(\mu)}$ are computed as usual. The remaining grid point fields to be used in (4.93), namely $U^{(\mu)}$ and $V^{(\mu)}$ are obtained by computing at first grid point values of $\hat{\zeta}$ and $\hat{\delta}$ (using 4.104a and 4.104b) and then the relationships

$$\hat{U}^{(\mu)} = (1-\mu^2)\hat{\zeta} - \hat{V}^{(\mu)},$$
$$\hat{V}^{(\mu)} = -(1-\mu^2)\hat{\delta} + \hat{U}^{(\lambda)}.$$

The right hand sides of (4.93) can then be computed in the transform grid.

The inverse transforms back to spectral space of the tendencies of $\hat{\phi}$ proceed as usual, i.e. as shown in Section 4.5.2, whereas a new approach is introduced by using (4.101) (multiplied by $-n(n+1)/a^2$) to obtain the spectral coefficients of the tendencies of vorticity and divergence.

A time extrapolation may then be performed in spectral space. As Ritchie's formulation is intended for semi-Lagrangian advection, which we shall not consider here, the time extrapolation is done partly in grid point space in his formulation. Concerning computational cost it may be noted that by the use of the transforms (4.101) for all (m,n) two more of the expensive Legendre transforms are needed in Ritchie's method than in that of *Eliasen et al.* (1970) described in Section 4.5.2. It has been shown, however, by *Temperton* (1991) that (4.101) may be computed with only two Legendre transforms instead of four. The transforms (4.101) were based on (4.97) which by use of (4.78) and (4.5a) may be written

$$\{\alpha(A,B\}_{m,n} = im\tilde{A}_{m,n} + nD_{m,n+1}\tilde{B}_{m,n+1} + 1 - (n+1)D_{m,n}\tilde{B}_{m,n-1}$$

where (4.112)

$$(\tilde{\ })_{m,n} = \tfrac{1}{2}\int_{-1}^{1}(\ )_m P_{m,n}(\mu)\, d\mu/(1-\mu^2).$$

When using this new expression (4.112) instead of (4.97) we get expressions corresponding to (4.101) which involve only two Legendre transforms, namely:

$$(d\hat{U}/dt)_{m,n} = \tfrac{1}{2} \int_{-1}^{1} (dU_m/dt)P_{m,n}d\mu/(1-\mu^2)$$

and

$$(d\hat{V}/dt)_{m,n} = \tfrac{1}{2} \int_{-1}^{1} (dV_m/dt)P_{m,n}d\mu/(1-\mu^2).$$

It may be noted that when using a similar technique in Bourke's model the number of Legendre transforms can be reduced to that of the U and V models.

It is obvious that Ritchie's formulation must be equivalent to those of *Bourke* (1972) and *Eliasen et al.* (1970) which were presented in the previous Sections. This was shown explicitly by *Ritchie* (1988).

An alternative new version of the transform method based on a vector spherical harmonic representation of the vector wind components u and v were proposed by *Browning et al.* (1989). It was subsequently shown by *Temperton* (1991) that this new formulation was equivalent to the formulations considered above in the present and previous Sections. As stated by *Temperton* (1991): "This illustrates one of the nice features of the spectral method: although there is certainly more than one way to organize the computations, there is fundamentally no argument about what is to be done".

4.5.5 Baroclinic spectral models

At the present time most global atmospheric models used for weather forecasting and climate simulations are spectral models. The spectral representation in the horizontal direction has usually been combined with a discrete representation in the vertical direction, although spectral representations as well as a finite element representation have also been considered (see references at the end of Section 2).

When using a discrete representation in the vertical direction the extension to baroclinic models of the spectral method described above is rather straightforward. The equations in sigma- or hybrid-coordinates are used and generally vorticity, divergence, temperature, specific humidity, and the logarithm of surface pressure are chosen as prognostic variables.

Some terms in the equations, e.g. vertical advection terms, become triple products of the variables. Using triangular truncation such terms become truncated series with $n \leq 3N$ and in order to avoid aliased interactions the numbers of longitudes K_1 and latitudes K_2 in the transform grid must satisfy

$$K_1 \geq 4N+1, \qquad K_2 \geq (4N+1)/2 \quad . \tag{4.113}$$

For parallelogrammic truncations the corresponding numbers become

$$K_1 = 4M+1, \qquad K_2 = (4M+4J+1)/2 \quad . \tag{4.114}$$

The remaining non-linear terms in the non-adiabatic frictionless part of the prognostic equations are only quadratic products and require only numbers of longitudes and latitudes which satisfy (4.79) or (4.80).

As mentioned in the introduction it is a big advantage of the transform method that the parameterization of physical processes, which depends upon locally determined decisions, can be included in physical space in the transform grid points. Utilizing this possibility spectral multi-level models with advanced parameterization of physical and sub-truncation scale processes have been developed.

Based on experiments by *Bourke* (1974), *Hoskins and Simmons* (1975) the number of grid points in the transform grid are generally chosen to satisfy (4.79) and (4.80) and not (4.113) or (4.114). That is, only linear and quadratic terms are calculated alias-free whereas aliasing is allowed for triple terms and for the parameterization of physical processes, which introduce a non-linearity of higher degree than quadratic. The above mentioned experiments indicate that the effect of this aliasing is acceptable.

According to *Bourke et al.* (1977) who uses the rhomboidal truncation an increase of the number of points above that determined by the minimum satisfying equation (4.80) has a negligible effect. On the other hand a decrease of the number K_1 of points along all Gaussian latitudes below the minimum determined by (4.80) was found to give unsatisfactory results.

The effect of reducing the number of Gaussian latitudes below the limits determined by (4.80) was not investigated. If both K_1 and K_2 are reduced to the numbers required to give alias-free calculations of linear terms only, that is with triangular truncations to $K_1 = 2N+1$, $K_2 = N+1$, then one should expect non-linear instability at least in the absence of artificial damping of small scale waves. This

is indeed found to be the case. So, a shallow water model i.e. the model described by *Machenhauer and Rasmussen* (1972) is found to "explode" within a few time steps, when K_1 and K_2 are set equal to these values.

Although a general reduction of the number of points along the Gaussian latitude circles seems to give unsatisfactory results, experiments by the author *Machenhauer*, (1979) indicated that when a triangular truncation is used a certain reduction of points along latitude circles below the value $3N+1$ can be made in middle to higher latitudes without any significant change of the integration results. This could be expected, since the resolution given by a triangular truncated spectral representation is isotropic and uniform all over the globe, whereas the transform grid, with the same number of points at all latitude circles, is highly non-isotropic and non-uniform due to the convergence of the meridians towards the poles.

Recently *Hortal and Simmons* (1991) made experiments with a transform grid in which the number of points at the Gaussian latitudes were reduced in such a way that the grid length in the zonal direction became as large as possible when requiring that it does not exceed the standard grid length at the equator and that the number of points enables the use of a fast Fourier transform. They report on a saving in computational time between 20% and 25% for the TI06 ECMWF forecast model with no significant loss of accuracy compared with the use of the standard transform grid.

As explained in Subsection 4.4.4 the truncated spectral equations for inviscid non-divergent flow conserve the mean kinetic energy and the mean enstrophy. In numerical integrations of these equations non-conservation of the invariants can be due only to round-off errors and time truncation. In practice, it is found that the effect of these errors is very small even for very long period integrations (*Ellsaesser*, 1966). As a consequence the average two-dimensional wavenumber is very nearly conserved and an unlimited systematic energy cascade towards the highest wavenumbers n is not possible. Nevertheless, as noted in Subsection 4.4.4, a certain blocking of energy in the highest wavenumbers is not excluded if at the same time energy is transferred to low wavenumbers. That such a blocking does in fact occur was shown by *Puri and Bourke* (1974). Two 8 day integrations with rhomboidal truncations, $M=15$ and $M=36$, were compared. In both integrations the same initial field, derived from observed data, was used. The total kinetic energy in each zonal wavenumber m was considered as a function of m. A considerable blocking of energy in the $M=15$ integration in the region $m = 10$ to $m = 15$ was found already after 4 days of integration. The blocking is illus-

trated in Figure 11, which shows the energy spectra averaged over the whole 8 day integrations period. As expected, this blocking shows up even more strongly in the enstrophy spectrum. It was shown by *Gordon and Stern* (1974) that the blocking phenomenon occurs in a spectral shallow water model as well and apparently it was found also by *Bourke* (1974) in his multi-level model.

The blocking phenomenon is a result of neglecting interactions involving components outside the truncation limits. It is observed as a gradual increase of energy in the small scale components and occurs most strongly and at an earlier time in low resolution models than in high resolution models. Apparently a damping influence on the smallest scales retained is missing. When the amplitudes of the small scale components have grown to unrealistically large values, one should expect that eventually, through non-linear interactions, this will lead to serious errors of the large scale components.

As expected one finds that some parameterization of the scale selective damping influence of the components outside the truncation limits do improve the integration results and that such a parameterization is needed especially in longer range low resolution models. Even in short range forecasting *Bourke* (1974) finds that some parameterization is required to inhibit spectral blocking, when using a rhomboidal truncation with M = 15 (R15). How the parameterization is most effectively introduced is still an open question, the form and magnitude chosen vary widely in different spectral models. We shall mention some formulations which are often used. *Bourke* (1974) and *Gordon and Stern* (1974) add linear diffusion terms of the form $K_H \nabla^2( )$ to the prognostic equations, whereas *Simmons and Hoskins* (1978) use diffusion terms of the form $K_H \nabla^4( )$, which damp the small scale components more selectively. *Bourke* (1974) applies the diffusion only to components with n > M, i.e. for the components in the upper half of the rhombus in the m,n - diagram, and only in the prognostics for vorticity, temperature and logarithm of surface pressure. For divergence a linear dissipation term of the form $-K\delta$ is added, which serves the dual purpose of preventing blocking and suppressing spurious gravity oscillations. The above linear diffusion and dissipation terms are simple to include in a spectral model because of the property (4.13) of the spherical harmonics.

References

Arpe, K., 1976: Entwicklungen der Orographie der Erde nach Kugelflächenfunktionen. ECMWF Internal Paper.

Baede, A.P.M., D. Dent and A. Hollingsworth, 1976: The effect of arithmetic precision on some meteorological integrations. ECMWF Technical Report No. 2.

Baer, F., 1964: Integration with the spectral vorticity equation. J. Atmos.Sci., 21, 260-276.

Baer, F., 1972: An alternate scale representation of atmospheric energy spectra. J.Atmos.Sci., 29, 649-664.

Baer, F., and G.W. Platzman 1961: A procedure for numerical integration of the spectral vorticity equation. J.Meteor., 18, 393-410.

Belousov, S.L., 1962: Tables of normalized associated Legendre polynomials.

Bourke, W., 1972: An efficient, one-level, primitive-equation spectral model. Mon.Wea.Rev., 100, 683-689.

Bourke, W., 1974: A multi-level spectral model. I. Formulation and hemispheric integrations. Mon.Wea.Rev., 102, 687-701.

Bourke, W., K. Puri and R. Thurling, 1974: Numerical prediction for the Southern Hemisphere via the spectral method. GARP WGNE Report No. 7, 22-42.

Bourke, W., McAvaney, B. Puri, K. and Thurling R., 1977: Global modelling of atmospheric flow by spectral methods. Methods in computational physics. Vol. 17: General circulation models of the atmosphere. Ed. J.Chang, 267-324.

Browning, G.L., J.J. Hack and P.N. Swarztrauber, 1989: A comparison of three numerical methods for solving differential equations on the sphere. Mon.Wea.Rev., 117, 1058-1075.

Byrnak, B.P., 1975: An operational spectral semi-implicit one-layer model. The Danish Meteorological institute, Meddelelser Nr. 25.

Cooley, J.W., and J.W. Tukey, 1965: An algorithm for the machine calculation of complex Fourier series. Math.Comp., 19, 267-301.

Courant, R. and D. Hilbert, 1953: Methods of mathematical physics, Vol. I.

Craig, R., 1945: A solution of the nonlinear vorticity equations for atmospheric motion. J.Meteorol., 2, 175-178.

Daley, R., I. Simmons and J. Henderson, 1974: A Galerkin approach to short-term forecasting in the Northern Hemisphere. GARP WGNE Report No. 7, 43-45.

Daley, R., C. Girard, J. Henderson and I. Simmons, 1976: Short term forecasting with a multi-level spectral primitive equations model. Atmosphere, 14, 98-134.

Daley, R. and Y. Bourassa, 1978: Rhomboidal versus triangular spherical harmonic truncation: Some verification statistics. Atmosphere-Ocean, 16, 187-196.

Dickinson, R.E. and D.L. Williamson, 1972: Free oscillations of a discrete stratified fluid with application to numerical weather prediction. J.Atmos.Sci., 29, 623-640.

Doron, E., A. Hollingsworth, B.J. Hoskins, and A.J. Simmons, 1974: A comparison of grid-point and spectral methods in a meteorological problem. Quart.Journ.Roy.Met.Soc., 100, 371-383.

Eliasen, E. and B. Machenhauer, 1965: A study of the fluctuations of the atmospheric planetary flow patterns represented by spherical harmonics. Tellus, Vol. 17, 220-238.

Eliasen, E., Machenhauer, B., and Rasmussen, E., 1970: On a numerical method for integration of the hydrodynamical equations with a spectral representation of the horizontal fields. Report No. 2, Institut for teoretisk meteorologi, University of Copenhagen.

Eliasen, E., and B. Machenhauer, 1974: On the spectral representation of the vertical variation of the meteorological fields in numerical integrations of a primitive equations model. GARP WGNE Report No. 7, 83-93.

Ellsaesser, H.W., 1966: Evaluation of spectral versus grid methods of hemispheric numerical weather prediction. J.Appl.Meteor., 5, 246-262.

Ellsaesser, H.W., 1966: Expansion of hemispheric meterological data in anti-symmetric surface spherical harmonic (Laplace) series., J.Appl.Meteor., 5, 263-276.

Fjørtoft, R., 1953: On the changes in the spectral distribution of kinetic energy for two-dimensional, non-divergent flow. Tellus, 5, 225-230.

Flattery, T.W., 1970: Spectral models for global analysis and forecasting. Air Weather Service Technical Report 242.

Galerkin, B., 1915: Rods and plates. Series occuring in various questions concerning the elastic equilibrium of rods and plates. Vestnik Inzhenerov, 19, 897-908.

Gates, W.L. and A.B. Nelson, 1975: A new (revised) tabulation of the Scripps Topography on a 1° global grid. Part I: Terrain heights. Rand Corporation, R-1276-1-ARPA.

Girard, C. and M. Jarraud, 1982: Short and medium range forecast differences between a spectral and grid point model. An extensive quasi operational comparison. ECMWF Tech.Rep.No. 32, 117.

Gordon, T. and W. Stern, 1974: Spectral modelling at GFDL. GARP WGNE Report No. 7, 46-82.

Haurwitz, B., 1940: The motion of atmospheric disturbances on the spherical earth. J.Marine Res., 3, 254-267.

Hobson, E.W., 1955: Spherical and ellipsoidal harmonics.

Hortal, M. and A.J. Simmons, 1991: Use of Reduced Gaussian Grids in Spectral Models. Mon.Wea.Rev., 119, 1057-1074.

Hoskins, B.J. and A.J. Simmons, 1974: The development of spectral models in the UK University Atmospheric Modelling Group. GARP WGNE Report No. 7, 94-99.

Hoskins, B.J. and A.J. Simmons, 1975: A multi-layer spectral model and the semi-implicit method. Quart.J.Roy.Soc., 101, 637-655.

Jarraud, M. and A.J. Simmons, 1984: The Spectral Technique. Numerical Methods for Weather Prediction. ECMWF Seminar 1983, Volume 2, 1-59.

Jarraud, M. and C. Girard, 1984: An extensive quasi-operational comparison between a spectral and a grid point model. ECMWF Seminar 1983, Volume 2, 61-111.

Kasahara, A., 1977: Numerical integration of the global barotropic primitive equations with Hough harmonic expansions. J.Atmos.Sci., 34, 687-701.

Kasahara, A., 1978: Further studies on a spectral model of the global barotropic primitive equations with Hough harmonic expansions. J.Atmos.Sci., 35, 2043-2051.

Kreiss, H. and J. Oliger, 1973: Methods for the approximate solution of time dependent problems. WMO 11 CSU Joint Organizating Committee, GARP Publication Series No. 10.

Krylov, V.I., 1962: Approximate calculation of integrals.

Kubota, S., 1959: Surface spherical harmonic representations of the system of equations for analysis. Papers Meteor. Geophys. (Tokyo), Vol. 10, 145-166.

Kubota, S., M. Hirose, Y. Kikuchi and Y. Kurihara, 1961: Barotropic forecasting with the use of surface spherical harmonic representation. Pap. Meteorol. Geophys., 12, 199-215.

Kwizak, H., and A. Robert, 1971: A semi-implicit scheme for grid point atmospheric models of the primitive equations. Mon.Wea.Rev., 99, 32-36.

Lorenz, E.N., 1960: Maximum simplification of the dynamic equations. Tellus, 12. 243-254.

Machenhauer, B., 1974: On the use of the spectral method in numerical integrations of atmospheric models. Proceedings of the Symposium on Difference and Spectral Methods for Atmosphere and Ocean Dynamics Problems, Sept. 1973. USSR Academy of Sciences, Siberian Branch, Novosibirsk.

Machenhauer, B., 1977: On the dynamics of gravity oscillations in a shallow water model, with application to nonlinear normal mode initialization. Beiträge zur Physik der Atmosphäre, 50, 253-271.

Machenhauer, B., 1979: The spectral method. Numerical methods used in atmospheric models. GARP publication series No. 17, 121-275.

Machenhauer, B. and R. Daley, 1972: A baroclinic primitive equation model with a spectral representation in three dimensions. Institute of Theoretical Meteorology, University of Copenhagen, Report No. 4.

Machenhauer, B. and R. Daley, 1974: Hemispheric spectral model. GARP Publication Series No. 14, 226-251.

Machenhauer, B. and Rasmussen, E., 1972: On the integration of the spectral hydrodynamical equations by a transform method. Report No. 3, Institut for teoretisk meteorologi, University of Copenhagen.

Merilees, P.E., 1966: Harmonic representation applied to large scale atmospheric waves. A.M.R.G. Publication in Meteorology, 83.

Merilees, P.E., 1968: Equations of motion in spectral form. J.Atmos.Sci., 25, 736-743.

Merilees, P.E., 1972: Truncation error in a spectral model. Atmosphere, 10, 1-9.

Merilees, P.E., 1973: An alternative scheme for summation of a series of spherical harmonics. J.Appl.Meteor., 12, 224-227.

Neamtan, S.M., 1946: The motion of harmonic waves in the atmosphere. J.Meteor., 3, 53-56.

Neumann, F., 1838: Über eine neue Eigenschaft der Laplaceschen $Y^{(n)}$ und ihre Anwendung zur analytischen Darstellung derjenigen Phänomene, welche Funktionen der geographischen Länge und Breite sind. Schumachers Astron.Nachr., 15, 313-325. (Reprinted in Math.Ann., 14, p.567).

Orszag, S.A., 1970: Transform method for calculation of vector-coupled sums: Application to the spectral form of the vorticity equation. J.Atmos.Sci., 27, 890-895.

Orszag, S.A., 1971: Numerical simulations of incompressible flows within simple boundaries: Accuracy. J.Fluid Mech., 49, 75-112.

Orszag, S.A., 1974: Fourier series on spheres. Mon.Wea.Rev., 102, 56-75.

Orszag, S.A., 1979: Spectral methods for problems in complex geometrics. Numerical methods for partial differential equations. Edited by S. Porter.

Phillips, N.A., 1959: An example of non-linear computational instability. The Atmosphere and the Sea in motion, Rossby Memorial Volume, New York, Rockefeller Instit., 501-504.

Platzman, G.W., 1960: The spectral form of the vorticity equation. J.Meteor., 17, 635-644.

Platzman, G.W., 1961: An approximation to the product of discrete functions. J.Meteor., 18, 31-37.

Platzman, G.W., 1964: An exact integral of complete spectral equations for unsteady one-dimensional flow. Tellus, 16, 422-431.

Puri, K. and W. Bourke, 1974: Implications of horizontal resolution in spectral model integrations. Mon.Wea.Rev., 102, 333-347.

Rectory, K., 1969: Survey of applicable mathematics. Iliffe Books Ltd.

Ritchie H., 1988: Application of the semi-Langrangian method to a spectral model of the shallow water equations. Mon.Wea.Rev., 116, 1587-1598.

Robert, A.J., 1966: The integration of a low order spectral form of the primitive meteorological equations. J.Meteor.Soc. Japan, 44, 237-244.

Silberman, I., 1954: Planetary waves in the atmosphere. J.Meteor., 11, 27-34.

Simmonds, I., 1975: The spectral representation of moisture. J.Appl.Meteor., 14, 175-179.

Simmonds, A.J. and B.J. Hoskins, 1975: A comparison of spectral and finite-difference simulations of a growing baroclinic wave. Q.J.Roy.Meteor.Soc., 101, 551-565.

Simmons, A.J. and B.J. Hoskins, 1978: The life cycles of some non-linear baroclinic waves. J.Atmos.Sci., 35, 414-432.

Simmons, A.J. and Burridge, D.M., 1981: An energy and angular momentum conserving vertical finite difference scheme and hybrid vertical coordinate. Mon.Wea.Rev., 109, 758-766.

Stainforth, A.N. and R. Daley, 1977: A finite-element formulation for the vertical discretization of sigma-coordinate primitive equation models. Mon.Wea.Rev., 105, 1108-1118.

Temperton, C., 1991: On Scalar and Vector Transform Methods for Global Spectral Models. Mon.Wea.Rev., 119, 1303-3107.

Weigle, W.F., 1972: Energy conservation and the truncated spectral form of the primitive equations for a one-layer fluid. NCAR cooperative thesis No. 26, University of Michigan and Laboratory of Atmospheric Science, NCAR.

Williamson, D.L. and R.E. Dickinson, 1976: Free oscillations in the NCAR global circulation model. Mon.Wea.Rev., 104, 1372-1391.